



Investigation of Use of Lead Oxide Extracted from Recycled Batteries in Radar Absorbing Stealth Technology

Submitted to the Graduate School of Natural and Applied Sciences
in partial fulfillment of the requirements for the degree of

Doctor of Philosophy

in Material Science and Engineering

by

Gürkan Ergün

ORCID 0000-0002-9140-8540

June 2023

This is to certify that we have read the thesis **Investigation of Use of Lead Oxide Extracted from Recycled Batteries in Radar Absorbing Stealth Technology** submitted by **Gürkan Ergün**, and it has been judged to be successful, in scope and in quality, at the defense exam and accepted by our jury as a DOCTORAL THESIS.

APPROVED BY:

Advisor:

Assoc. Prof. Dr. Gül Yılmaz Atay
İzmir Kâtip Çelebi University

Committee Members:

Assoc. Prof. Dr. Ömer Faruk Ebeođlugil
Dokuz Eylul University

Assoc. Prof. Dr. Onur Ertuđrul
İzmir Kâtip Çelebi University

Date of Defense: June 23, 2023

Declaration of Authorship

I, **Gürkan Ergün**, declare that this thesis titled **Investigation of Use of Lead Oxide Extracted from Recycled Batteries in Radar Absorbing Stealth Technology** and the work presented in it are my own. I confirm that:

- This work was done wholly or mainly while in candidature for the Doctoral degree at this university.
- Where any part of this thesis has previously been submitted for a degree or any other qualification at this university or any other institution, this has been clearly stated.
- Where I have consulted the published work of others, this is always clearly attributed.
- Where I have quoted from the work of others, the source is always given. This thesis is entirely my own work, with the exception of such quotations.
- I have acknowledged all major sources of assistance.
- Where the thesis is based on work done by myself jointly with others, I have made clear exactly what was done by others and what I have contributed myself.

Date: 23.06.2023

Investigation of Use of Lead Oxide Extracted from Recycled Batteries in Radar Absorbing Stealth Technology

Abstract

Radar is the most common technique for the detection and tracking of aircraft. Although radar is an indispensable tool in aviation traffic management, it is a problem in offensive military operations which require aircraft to attack their target and then escape without being detected. Radar involves the transmission of electromagnetic waves into the atmosphere; they are then reflected off the aircraft back to a receiving antenna. Radar Absorbing Materials (RAM) works on the principle of the aircraft absorbing the electromagnetic wave energy to minimize the intensity of the reflected signal. The development of radiation absorbing materials, which provides stealth technology, where privacy and invisibility are extremely vital, is of great importance. At the same time, the use of wasted batteries in the production of Radar-absorbing materials will play a very valuable role. In addition, the recovery of lead decreases the lead dispersion in the environment and preserves the mineral reserves for the future.

In this thesis, radar absorption material with lead oxide which we obtained from recycling car batteries, was investigated. First, Lead Oxide extracted from the plates of the recycled car battery. The chemical, magnetic (VSM), structural (XRD), particle size and electron microscope (SEM) analyses were performed before constructing RAMs.

After obtaining lead oxide from car battery recycling, the next step is to continue with grinding it and filtering from sieves in different particle sizes. After categorizing the samples with respect to their size, Radar absorbing samples were prepared by adding and pressing the obtained lead and lead oxide products at different rates between the polyurethane foam. Network analyzer tests were carried out to determine the radar absorbing properties of the composites by using PNA-L Network Analyzer. As a

result, very low reflection coefficients and moderately acceptable transmission coefficients were found with different types of designed RAMs manufactured with Lead Oxide.

Keywords: Stealth technology, Radar, RAMs, Lead Oxide, characterization, recycling batteries, Network Analyzer

Atık Pillerden Elde edilen Kurşun Oksidin Radar Emici Gizlilik Teknolojisinde Kullanımının İncelenmesi

ÖZ

Radar, uçakların tespiti ve takibi için en yaygın tekniktir. Radar, havacılık trafik yönetiminde vazgeçilmez bir araç olmasına rağmen, uçağın hedefini saldırıp fark edilmeden kaçmasını gerektiren saldırgan askeri operasyonlarda sorun oluşturur. Radar, elektromanyetik dalgaların atmosfere yayılmasını içerir; daha sonra uçaktan yansarak bir alıcı antene geri döner. Radar Emici Malzemeler (RAM), uçağın elektromanyetik dalga enerjisini emerek yansıyan sinyalin yoğunluğunu en aza indirmesi prensibiyle çalışır. Gizlilik ve görünmezlik gibi son derece önemli olan gizlilik teknolojisini sağlayan radyasyon emici malzemelerin geliştirilmesi büyük önem taşır. Aynı zamanda, atık pillerin Radar emici malzemelerin üretiminde kullanılması, çok değerli bir rol oynayacaktır. Ayrıca, kurşunun geri kazanılması, kurşun dağılımını çevrede azaltır ve mineral rezervlerini gelecek için korur.

Bu tezde, geri dönüştürülen araba pillerinden elde ettiğimiz kurşun oksit ile radar emici malzeme incelenmiştir. İlk olarak, geri dönüştürülen araba pilinin plakalarından Kurşun Oksit çıkarılmıştır. Kimyasal, manyetik (VSM), yapısal (XRD), parçacık boyutu ve elektron mikroskobu (SEM) analizleri, RAM'ların yapımından önce gerçekleştirilmiştir.

Atık pillerden elde edilen kurşun oksidin elde edilmesinden sonra, bir sonraki adım, farklı parçacık boyutlarında elekten öğütülmesi ve süzülmesiyle devam etmektedir. Örnekler, boyutlarına göre kategorize edildikten sonra, elde edilen kurşun ve kurşun oksit ürünleri poliüretan köpük arasına farklı oranlarda eklenerek ve sıkıştırılarak Radar emici örnekler oluşturulmuştur. Radar emici bileşiklerin radar emici özelliklerini belirlemek için PNA-L Ağ Analizörü kullanılarak ağ analizör testleri yapılmıştır. Sonuç olarak, kurşun oksit ile üretilen farklı tiplerde tasarlanmış

RAM'lerin çok düşük yansımaya katsayıları ve kabul edilebilir düzeyde iletim katsayıları bulunmuştur.

Anahtar Kelimeler: Gizlilik teknolojisi, Radar, RAM'ler, Kurşun Oksit, karakterizasyon, pil geri dönüşümü, Ağ Analizörü

This thesis work is to be dedicated to my son Mikael, my mother, and my advisor...

Acknowledgment

I would like to thank Alper Turhan for his material supply. I also thank my advisor Gül Yılmaz Atay.

Table of Contents

Declaration of Authorship	II
Abstract	III
Öz	V
Acknowledgment	VIII
Table of Contents	IX
List of Figures	XI
List of Tables	XV
List of Abbreviations	XVI
List of Symbols	XVII
Chapter 1	1
Introduction	1
1.1 Radar and Radar Absorption	1
1.2 Lead Oxide	3
1.3 Lead-Acid Batteries and The Importance of Their Recycling for Radar Absorbing Materials	4
1.4 Network analyzer and S-Parameters	7
Chapter 2	9
Experimental Part	9
2.1 Preparation of Lead Oxide by Recycling Car Battery	9

2.2 Characterization of Recycled Lead Oxide	12
2.2.1 Chemical Analysis	12
2.2.2 Color Indication	12
2.2.3 Scanning Electron Microscopy (SEM)	13
2.2.4 VSM (Vibrating-Sample Magnetometer)	15
2.2.5 The Particle Size Analysis	18
2.2.6 X-Ray Diffraction	20
Chapter 3.....	26
Materials and Methods	26
3.1 Filtering.....	26
3.2 The Design of RAMs.....	27
3.2.1 Styrofoam.....	27
3.3 Vector Network Analyzer (VNA) Measurements	28
Chapter 4.....	31
Results and Discussions	31
4.1 VNA Results.....	31
Chapter 5.....	58
Conclusion.....	58
References	60

List of Figures

Figure 2.1: The extraction process of lead oxide plates from the car battery.	11
Figure 2.2: Lead Oxide extraction from the plates by using a simple tweezer.	11
Figure 2.3: SEM images from the bottom part of the lead oxide plate samples.	13
Figure 2.4: SEM images from the middle part of the lead oxide plate samples.	14
Figure 2.5: SEM images from the upper part of the lead oxide plate samples.	15
Figure 2.6: VSM result of the top part of the lead oxide plate sample.	16
Figure 2.7: VSM result of the middle part of the lead oxide plate sample.	16
Figure 2.8: VSM result of the lower part of the lead oxide plate sample.	17
Figure 2.9: VSM result of the Styrofoam (no sample).....	18
Figure 2.10: The particle size analysis result of the top part of the lead oxide plate sample.	19
Figure 2.11: The particle size analysis result of the top part of the lead oxide plate sample.	20
Figure 2.12 The XRD of the spent lead paste before calcination. [44].....	22
Figure 2.13 The XRD results of the non-grinded (above) and grinded (below) powder from the recycled battery.	24
Figure 3.1: Vibratory Sieve Shaker (Retsch)	26
Figure 3.2: Single, double, and triple layered RAMs - combination of styrofoam (white colored) and lead oxide sample (brown colored).	27

Figure 4.1: S ₁₁ for the non-grinded lead oxide powder inside a paper matchbox. Black 50 mg, Red 100 mg, Blue 150 mg.	31
Figure 4.2: S ₂₁ for the non -grinded lead oxide powder inside a paper matchbox (see above). Black 50 mg, Red 100 mg, Blue 150 mg.	32
Figure 4.3: S ₁₁ for empty and different amounts of the non - grinded lead oxide powder inside a single styrofoam.....	33
Figure 4.4: S ₂₁ for empty and different amounts of the non -grinded lead oxide powder inside a single styrofoam.....	33
Figure 4.5: S ₁₁ for the same (100 mg) amount of the grinded lead oxide powder inside a single styrofoam with different particle size: the smaller than 75 micron and the sample taken from the bottom part of the plate - black, between 75 micron and 130 micron - red (the sample taken from the top part of the plate), greater than 130 micron - blue (the sample taken from the top part of the plate).	34
Figure 4.6: S ₂₁ for the same (100 mg) amount of the grinded lead oxide powder inside a single styrofoam with different particle size: the smaller than 75 micron and the sample taken from the bottom part of the plate - black, between 75 micron and 130 micron - red (the sample taken from the top part of the plate), greater than 130 micron - blue (the sample taken from the top part of the plate).	35
Figure 4.7: S ₁₁ for the Single and double layered lead oxide (the particle size bigger than 130 micron).	36
Figure 4.8: S ₁₁ and S ₂₁ for the single and triple layered styrofoam RAM samples which contain the same total amount of lead oxide (the particle size is bigger than 130 micron).	37
Figure 4.9: S ₁₁ and S ₂₁ for the double and triple layered styrofoam RAM samples which contain different amounts of lead oxide (the particle size is bigger than 130 micron).	37
Figure 4.10: S ₁₁ and S ₂₁ for the double layered RAMs with different particle sizes (below and above 75 micron).....	38

Figure 4.11: S_{11} and S_{21} can be seen for different amounts of lead oxide in a single layered RAM for the same particle size (below 75 micron)	39
Figure 4.12: S_{11} and S_{21} for the single layer RAMS with different amounts of lead oxide in the same particle size (above 75 micron).....	40
Figure 4.13: Comparison of lead oxide powder. The smaller particle size (below 25 micron) looks much more reddish (left) and the greater particle size (above 135 micron) looks completely brown.	42
Figure 4.14: S_{11} and S_{21} for the single layer RAM with the same amount of lead oxide in the same particle size (below 25 micron) versus sellotape (adhesive tape).....	44
Figure 4.15: S_{11} and S_{21} for the single layer RAM which contains 100 mg lead oxide.	45
Figure 4.16: S_{11} and S_{21} for the double layered RAM which contains 200 mg lead oxide in total.....	46
Figure 4.17: S_{11} and S_{21} for the single layer RAM which contains 200 mg lead oxide in total.....	47
Figure 4.18: The preparation of epoxy with 3 % stiffener	49
Figure 4.19: Graphite and coal powders are prepared until maximum value 3 % inside the mixture of epoxy.	50
Figure 4.20: The waveguide molds are filled by the epoxy mixture.	50
Figure 4.21: S_{11} and S_{21} for constant amounts of Graphite with changing amounts of PbO_2 with particle size below 25 microns inside the epoxy.	52
Figure 4.22: S_{11} and S_{21} for constant amounts of Graphite with changing amounts of PbO_2 with particle size above 75 micron inside the epoxy.....	52
Figure 4.23: S_{11} and S_{21} for constant amounts of coal with changing amounts of PbO_2 with particle size below 25 microns inside the epoxy.....	53

Figure 4.24: S_{11} and S_{21} for constant amounts of coal with changing amounts of PbO_2 with particle size above 75 microns inside the epoxy.....	54
Figure 4.25: S_{11} and S_{21} for changing amounts of graphite with constant amounts of PbO_2 with particle size below 25 microns inside the epoxy.	55
Figure 4.26: S_{11} and S_{21} for changing amounts of coal with constant amounts of PbO_2 with particle size below 25 microns inside the epoxy.....	56
Figure 4.27: S_{11} and S_{21} for changing amounts of graphite with constant amounts of PbO_2 with particle size above 75 microns inside the epoxy.	57

List of Tables

Table 1.1 List of Dielectric/Semiconducting RAMs for Broadband Absorption.. 5

List of Abbreviations

RAM	Radar Absorbing Material
İKÇÜ	İzmir Kâtip Çelebi University
PbO	Lead Oxide
ORCID	Open Researcher and Contributor ID
PE	Polyethylene

List of Symbols

S_{11}	Reflection Coefficient
S_{21}	Transmission Coefficient

Chapter 1

Introduction

1.1 Radar and Radar Absorption

Radar, an ingenious technology harnessing radio waves, proves invaluable in detecting and precisely locating objects. Originating during the tumultuous era of World War II, its initial deployment focused on military applications, yet its influence has significantly expanded to encompass domains like aviation, meteorology, and navigation. In this thesis, an intricate examination of radar technology is presented, encompassing its fundamental principles, operational mechanisms, and versatile applications.

The term 'radar' is an abbreviation of 'radio detection and ranging.' It operates by emitting a radio signal that travels through the atmosphere and bounces back after hitting any object in its path. The radar receiver captures this reflected signal, referred to as an 'echo,' and then processes it to ascertain the location, speed, and other characteristics of the object. Measuring the time delay between signal transmission and reception allows calculating the object's distance, while the Doppler shift of the echo helps determine its velocity.

There exist different categories of radar systems, encompassing pulse radar, continuous-wave (CW) radar, and frequency-modulated continuous-wave (FMCW) radar. The functioning of pulse radar entails the transmission of brief radio wave pulses, subsequently evaluating the temporal gap between the transmitted and received signals [1]. Conversely, CW radar emits a nonstop wave and gauges the alteration in frequency

of the reflected signal caused by the Doppler effect [2]. FMCW radar, an iteration of CW radar, employs a frequency that undergoes constant modification to determine the distance to the targeted object [3].

Radar technology boasts a myriad of applications across diverse domains. Take aviation, for example, where radar serves crucial roles in air traffic control, weather surveillance, and collision avoidance systems [4]. Meteorology heavily relies on radar for the identification and monitoring of storms, precise measurement of precipitation, and comprehensive examination of atmospheric phenomena [5]. Likewise, navigation leverages radar for adeptly guiding ships and boats, swiftly detecting obstacles, and accurately mapping coastlines [6].

Stealth technology involves a fascinating phenomenon known as radar absorption. It pertains to the absorption of electromagnetic waves, often in the microwave or radio frequency spectrum, by certain materials. This phenomenon finds applications across diverse domains, ranging from military advancements to the intriguing realm of materials science. The following academic discourse delves into the theoretical foundations of radar absorption, encompassing its core principles, real-world applications, and ongoing explorations in current research.

The absorption of radar waves depends primarily on the dielectric properties of the material under consideration. Dielectric materials possess the unique characteristic of efficiently storing and discharging electrical energy, which directly influences their capacity to absorb electromagnetic radiation. As radar waves interact with a dielectric substance, the electric dipole moments of the material react to the electric field accompanying the wave, resulting in the material's temperature elevation and subsequent absorption of the wave's energy [7].

The energy absorption of a material is influenced by several factors, encompassing the frequency of the radar wave, the material's thickness, and composition, as well as the angle at which the wave approaches. Broadly speaking, materials exhibiting high dielectric constants and significant loss tangents demonstrate superior radar wave absorption compared to materials with low dielectric constants and minimal loss tangents [8].

There exist numerous real-world implementations of radar absorption, especially within military advancements. Notably, the creation of stealth aircraft involves the integration of substances capable of effectively absorbing radar signals, thus enabling evasion of detection. The realm of military also encompasses additional utilities such as radar-absorbing coatings intended for usage on naval vessels and land vehicles. Moreover, absorptive materials are employed within antennas and various electronic components for their radar-attenuating properties [9].

Furthermore, apart from its prominent role in military applications, radar absorption holds substantial implications in materials science and engineering. For instance, scientists are actively exploring the potential of radar-absorbing materials for effective electromagnetic interference shielding. Additionally, they are focusing on innovating novel materials tailored for electronic devices and sensors [10].

1.2 Lead Oxide

Lead oxide represents a chemical compound denoted by the formula PbO . Another term used for this compound is lead (II) oxide or plumbous oxide. While lead oxide can be found naturally as the mineral litharge, its more prevalent form is synthetically generated by subjecting lead metal to heat in the presence of air [11].

Lead oxide holds significant importance as an industrial chemical, finding diverse applications across various industries. It acts as a pigment, adding color to paints, serves as a stabilizer in plastics, and functions as an additive in rubber products [12]. Moreover, it plays a crucial role in the manufacturing of lead-acid batteries, widely utilized in the automotive sector and numerous backup power applications [13].

Researchers have discovered that lead oxide poses a threat to both human beings and animals due to its toxic nature. Prolonged exposure to lead oxide can lead to various health issues, notably affecting neurological and developmental aspects [14]. Consequently, numerous nations have imposed restrictions on the usage of lead oxide, prompting endeavors to explore safer substitutes.

Regarding its composition, lead oxide possesses a crystal structure that exhibits two variations: tetragonal and cubic. The specific structure formed depends on the

temperature during synthesis [15]. At lower temperatures, the tetragonal structure is more stable, whereas at higher temperatures, the cubic structure takes precedence. Lead oxide can be classified as an ionic compound, wherein the lead ion carries a +2 charge, and the oxide ion holds a -2 charge. The attractive force between these ions is an ionic bond, a type of chemical bonding that occurs between ions with opposing charges.

1.3 Lead-Acid Batteries and The Importance of Their Recycling for Radar Absorbing Materials

Given our nation's strategic position, the significance of defense systems cannot be overstated. The advancement of radiation-absorbing materials, essential for the development of stealth technology, plays a critical role in ensuring utmost privacy and invisibility. Simultaneously, leveraging discarded batteries in the manufacturing process of radar-absorbing materials (RAMs) holds immense value. This thesis delves into the exploration of lead oxide, derived from recycled car batteries, as a radar absorption material.

Approximately 60% of the batteries sold on a global scale fall under the category of lead-acid batteries. Recycling lead, which is a relatively straightforward process, accounts for the creation of the final product (secondary lead) that exhibits identical properties to primary lead derived from ore. Recycling and repurposing contribute to nearly 50% of the world's lead consumption. The major advantage of reclaiming metals from scrap lies in its simplicity and lower energy requirements compared to the production of primary lead from ores. In fact, the energy needed to generate recovered lead is 35–40% less than what is required for manufacturing lead from ore.

The process of lead recovery not only aids in safeguarding potential mineral reserves but also minimizes the dispersion of lead in the environment. It is estimated that a significant portion, approximately 85%, of the consumed lead can be effectively recycled. [16]

One of the primary concerns in aircraft technology involves the assessment of radar cross section (RCS) using broadband spectrum radar. In pursuit of reducing the reflective properties of traditional metallic aircraft structures, researchers are dedicating

considerable effort to develop radar absorption structures (RAS) based on polymer matrix composites (PMCs) with low RCS. The cutting-edge advancements in RAS involve sophisticated combinations of RAMs (radar absorbing materials) alongside multilayered grid devices, such as frequency selective surfaces, circuit analog absorbers, and metamaterials. These innovations aim to enhance the mechanical attributes of RAS, thereby ensuring superior performance in stealth aircraft. The successful realization of RAS using RAMs as fillers has paved the way for extensive research into achieving state-of-the-art stealth capabilities [17].

Numerous researchers are actively developing broadband stealth composite constructions using various techniques. Radar-absorbing structures (RAS) offer dual functionality, serving as load-carrying components while facilitating radar absorption. Techniques like radar absorbing fillers, incorporation of frequency selective surfaces (FSS) such as multilayered grid devices, metamaterials, and Circuit Analog (CA) absorbers are employed to fine-tune the electromagnetic (EM) properties of RAS. These fillers take on particulate (powder, flakes, or spheres) and fibrous forms, composed of conducting, magnetic, dielectric, and magneto-dielectric materials. The observed radar absorption fillers encompass a diverse range of carbon-based materials, including conducting carbon black (CCB), carbon fibers, single- and multi-walled carbon nanotubes, graphene, and reduced graphene oxides, among others. The losses incurred by these fillers in conduction, absorption, dielectric, and magnetic fields all contribute to effective attenuation. It is shown in the Table 1.1 below. [18]

Table 1.1: List of Dielectric/Semiconducting RAMs for Broadband Absorption.[18]

RAM fillers	Type	Frequency (GHz)	Max. reflection loss (dB)
Carbon black and short carbon fibers	Semiconducting and conducting	8-12	27
Foliated graphite nanocomposites (FGN)	Semiconducting	1-18	37
Short carbon fiber	Conducting	8.2-12.4	7-11
Carbon black, carbon fiber, multiwalled carbon nano tubes	Semi conducting and conducting	8-18	35
Conducting carbon black	Semiconducting	8.2-12.4	55
Carbon nano tubes	Semiconducting	2-18	24.27
Carbon nano tubes, reduced graphene oxide	Magnetic, dielectric	2-18 GHz	55
Graphene	Dielectric	2-18 GHz	37.8
Reduced graphene oxide	Dielectric	2-18 GHz	10-57
Carbon, reduced graphene oxide	Dielectric	2-18 GHz	38.8
Carbon nano fibers, fullerenes, micro-sized granular graphite, Single walled and multiwalled carbon nanotubes	Semiconducting/ conducting	8.2-12.4	10
Carbon black	Conducting		22.2
Multiwalled carbon nanotubes	Semiconducting	8-12	30

In theory, one of the most effective absorbers is a material with a heavy nucleus, such as lead. (Greater nucleus weight enhances absorption capabilities.) Consequently, lead finds widespread application in radiation protection for X-rays, gamma radiation, and nuclear power plants. Additionally, Lead Oxide, particularly when integrated into composites (e.g., PbO in glasses), serves as an agent to amplify a minute fraction of the initial signal, which is redirected towards the receiver [19]. Hence, in the realm of military aircraft, the incorporation of sharp edges is employed to disperse incoming radar waves effectively.

An alternate approach revolves around dispersed loading and encompasses the application of a radar-absorbing substance to coat the surface. Specifically, anechoic chamber walls have been treated with specialized radar absorbing materials (RAM) to effectively mitigate or hinder electromagnetic reflections originating from massive structures such as airplanes, ships, and tanks. [20]

RAMs, or Radar Absorbing Materials, exhibit artificial permittivity and/or permeability components. These specially designed coatings undergo modifications in their electrical and/or magnetic properties, enabling them to absorb radar energy selectively or broadly

across specific frequencies. The level of absorption at a given radar wave frequency is contingent upon the unique composition of the coating.

In the 1930s, the exploration of electromagnetic wave absorbers commenced, and the first patent for such a device was granted in the Netherlands back in 1936. This particular absorber took the form of a quarter-wave resonant type, utilizing titanium dioxide as a high permittivity material and carbon black for lossy resistance. Traditional dielectric absorber materials, like foams, polymers, and elastomers, typically lack magnetic characteristics. However, to modify the permeability of the base materials, magnetic substances such as ferrites, iron, and cobalt-nickel alloys are employed as exemplifications. Additionally, the dielectric properties can be altered by introducing high dielectric materials like carbon, graphite, and metal flakes [21]. This study marks the first-time combination of Lead oxide and Foam for research.

A substantial amount of PbO plays a crucial role in glass production. Its incorporation enhances the electrical resistivity, refractive index, and X-ray absorption properties of glass, contributing significantly to its overall improvement. The addition of PbO not only renders industrial ceramics and glass more electrically and magnetically inert but also serves the purpose of preventing X-ray emission in cathode ray tube glass. As mentioned previously, the importance of lead in automotive lead-acid batteries directly correlates with its consumption (including the processing of PbO) corresponding to the number of vehicles.

1.4 Network analyzer and S-Parameters

Network analyzers serve as essential tools for assessing the frequency-dependent characteristics of electrical networks. These instruments find widespread application in electrical engineering and telecommunications, facilitating the evaluation of electronic devices and circuits, including filters, amplifiers, and antennas. The acquired data from network analyzers is typically conveyed using S-parameters, which consist of complex-valued scattering parameters, providing valuable insight into the amplitude and phase of both reflected and transmitted signals [22].

The S-parameters play a crucial role in determining the reflection and transmission coefficients of a network. The reflection coefficient, symbolized by Γ , quantifies the

power reflection from the network when a signal is applied to it. On the other hand, the transmission coefficient, represented by T , gauges the power transmitted through the network. Both Γ and T are characterized by complex values, contingent on the incident signal's frequency and the network's properties [23].

The computation of reflection and transmission coefficients can be achieved through the utilization of S-parameters, employing the subsequent equations:

$$\Gamma = S_{11} + (S_{11}S_{22} - S_{12}S_{21})/(1 - S_{22}) \quad (1.1)$$

$$T = S_{21}/(1 - S_{22}) \quad (1.2)$$

where S_{11} , S_{12} , S_{21} , and S_{22} are the four S-parameters that describe the behavior of the network. The complexity of their relationship with the reflection and transmission coefficients, along with their dependence on input and output impedance of the network [24], becomes evident through these equations.

The coefficients of reflection and transmission play a crucial role in the study and design of electrical networks. These quantities serve multiple purposes, such as assessing antenna performance, evaluating circuit impedance matching, and characterizing transmission line behavior. Additionally, they prove invaluable in the realm of microwave circuit design, as the circuit's efficiency hinges on the effective power transfer between its various components [25].

Chapter 2

Experimental Part

2.1 Preparation of Lead Oxide by Recycling Car Battery

The extraction of lead oxide plates from recycled batteries begins with cutting and removing the top portion of the battery (Figure 2.1a). Next, the lead oxide plates are removed from the Polyethylene (PE) separators, as shown in Figure 2.1b and Figure 2.1c. The battery contains 9 anode and 9 cathode plates. Then, the plates are immersed in water for one hour to ensure proper cleaning before the heating process (Figure 2.1d). Finally, the plates are placed in an oven set at 100°C (373 Kelvin) for 60 minutes to facilitate drying, as illustrated in Figure 2.1e.



(a)



(b)



(c)



(d)



(e)

Figure 2.1: The extraction process of lead oxide plates from the car battery.

Lead oxides that have dried out are prepared for extraction from their own plates. An everyday tweezer can be used to remove PbO from the plates since it is so mild and soft (Figs. 2.a and 2.b). There are three levels of categories on the plate. the top, lower, and middle sections. A plastic bag containing the extracted lead oxide powder is placed inside a crucible. The powder of three separate Lead Oxide samples is ready to be utilized for characterization after being beaten in the bag with a mallet.



(a)



(b)

Figure 2.2: Lead Oxide extraction from the plates by using a simple tweezer.

2.2 Characterization of Recycled Lead Oxide

2.2.1 Chemical Analysis

Sulfate (SO_4) precipitation is the first step in the materials' chemical examination. Sulfate analysis from plate; 10 g battery paste, referred to as the "sample," was removed from moisture by being placed in a moisture analyzer. The material was then placed in a beaker. After adding 100 ml of Na_2CO_3 and giving it a gentle swirl, the mixture was brought to a boil for 20 minutes. After the solution had finished boiling, it was transferred to a 500 ml volumetric flask and some water was added. The solution was then filtered and boiled one more. To neutralize the solution, concentrated HCl was added. 40 cc of BaCl_2 were added while the solution was boiling. The solution was filtered after some time had passed. The precipitate was placed in the crucible and baked for three hours at a temperature between 600 and 700 degrees Celsius. Finally, the amount of BaSO_4 was computed and the amount of residual ash on the crucible was measured. All analyses were performed in the İNCİ AKÜ facility in Manisa, Turkey.

2.2.2 Color Indication

Because the amount of electricity transmitted to the lower side decreases, there is more transformation where the current enters the battery plate from the top side because the longer the journey, the greater the loss. As a result, the higher portion functions better while the bottom portion functions less. The acid density in the battery varies as well. More acid has been concentrated in the lowest portion. The current-driven conversion of PbSO_4 to PbO_2 slows down as the acid density rises. As a result, less of the lower part is converted from PbSO_4 to PbO_2 , which causes the bottom part to undergo the "sulfation" mechanism.

The lower portion appears lighter in color because lead sulfate is white. The color changes to brown because the concentration of black PbO_2 and PbSO_4 is greater near the bottom. This entire process is repeated, as Alper Turhan's PhD thesis explains. [26]

2.2.3 Scanning Electron Microscopy (SEM)

Scanning Electron Microscopy technique was used in order to investigate particle size and close look at 3 different parts of the plate (upper, middle and bottom parts). All results were obtained in the Central Research Laboratory in Katip Çelebi University.

SEM Results for the bottom part samples

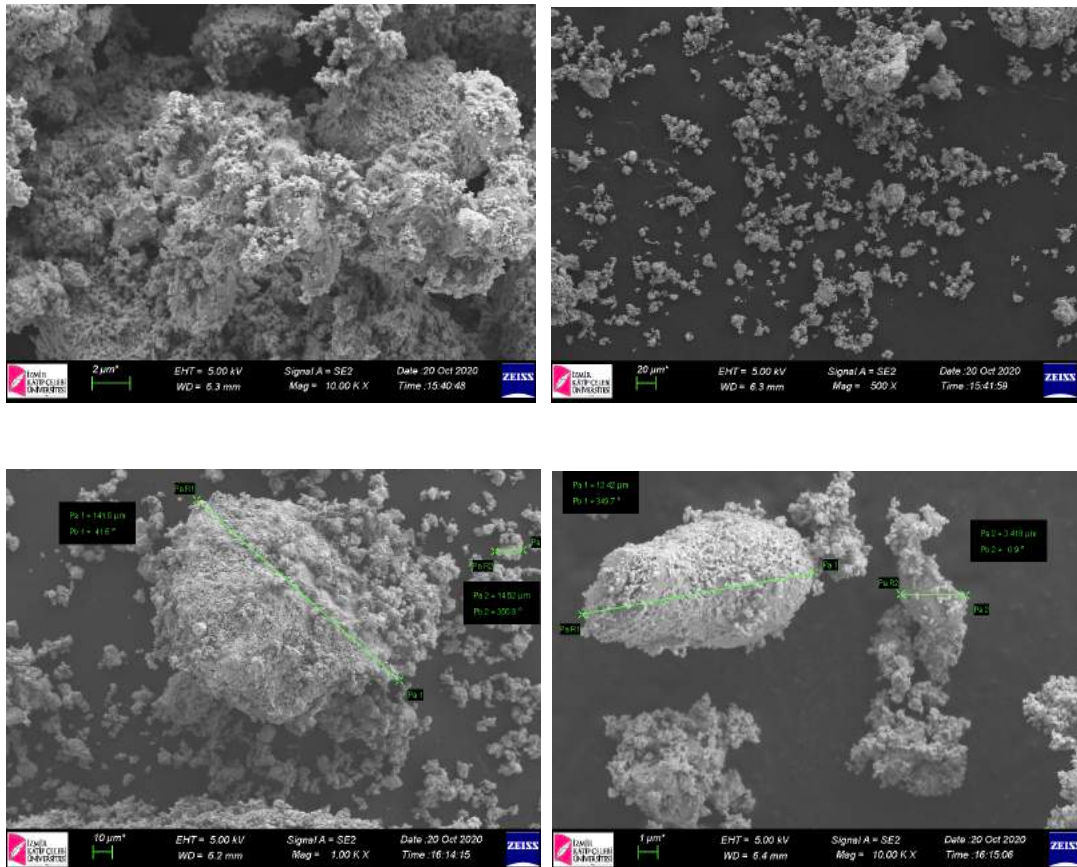


Figure 2.3: SEM images from the bottom part of the lead oxide plate samples.

SEM Results for the middle part samples

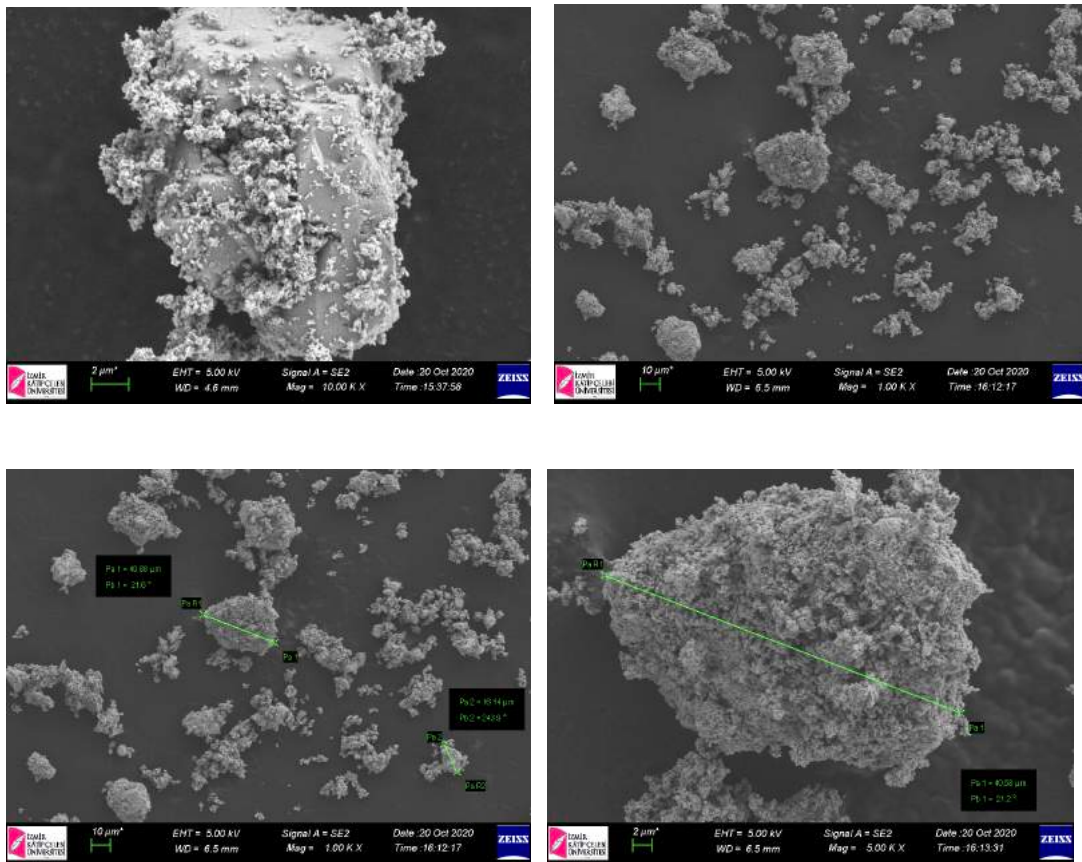


Figure 2.4: SEM images from the middle part of the lead oxide plate samples.

SEM Results for the upper part samples

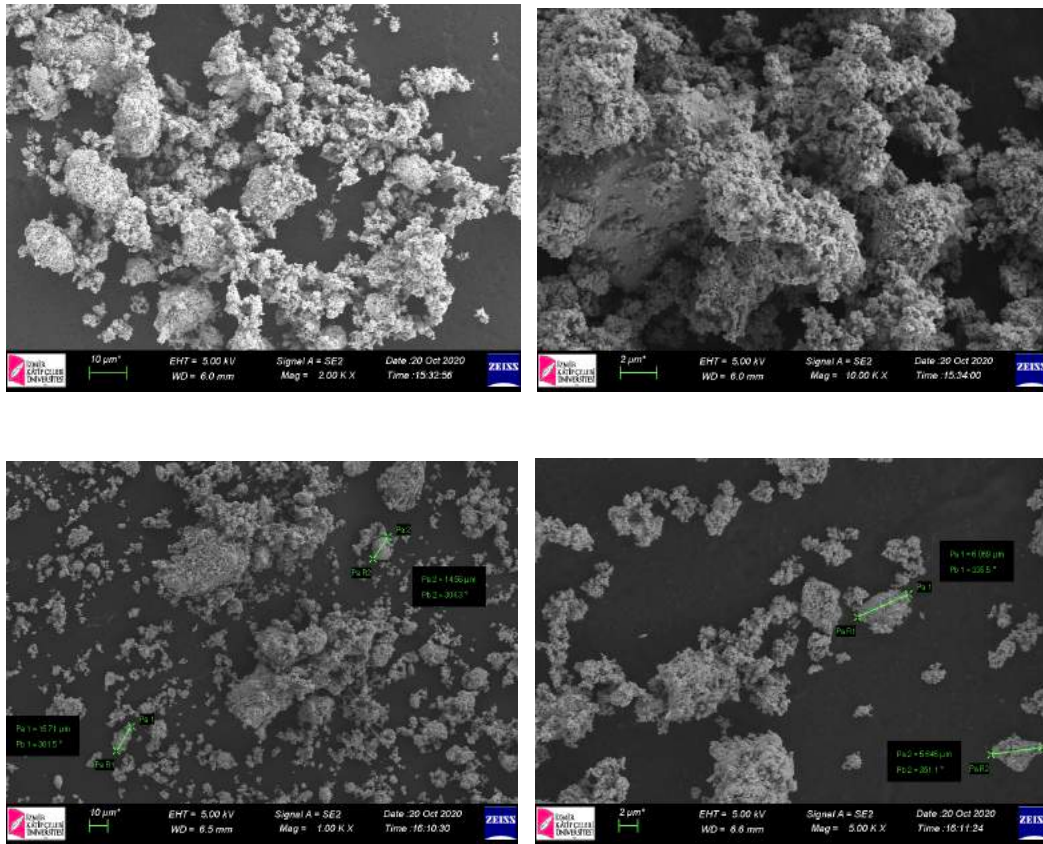


Figure 2.5: SEM images from the upper part of the lead oxide plate samples.

The SEM images show that there is wide range of distribution in size of the lead oxide particles. Since the particle size distribution contained enormous differences starting from nanoscale to microscale, the grinding process of the powder was planned.

2.2.4 VSM (Vibrating-Sample Magnetometer)

The process of VSM characterization offers valuable insights into the magnetic attributes of materials, encompassing key parameters like magnetic moment and susceptibility, which play a crucial role in RAMs design. RAMs are specifically engineered to transform radar frequency electromagnetic radiation into heat energy, making their magnetic properties directly proportional to their effectiveness.

By sweeping the magnetometer's magnetic field, hysteresis curves of three distinct PbO₂ recycling levels from the plates and styrofoam (for comparison) were also captured. Every observation made at Dokuz Eylül University's EMUM.

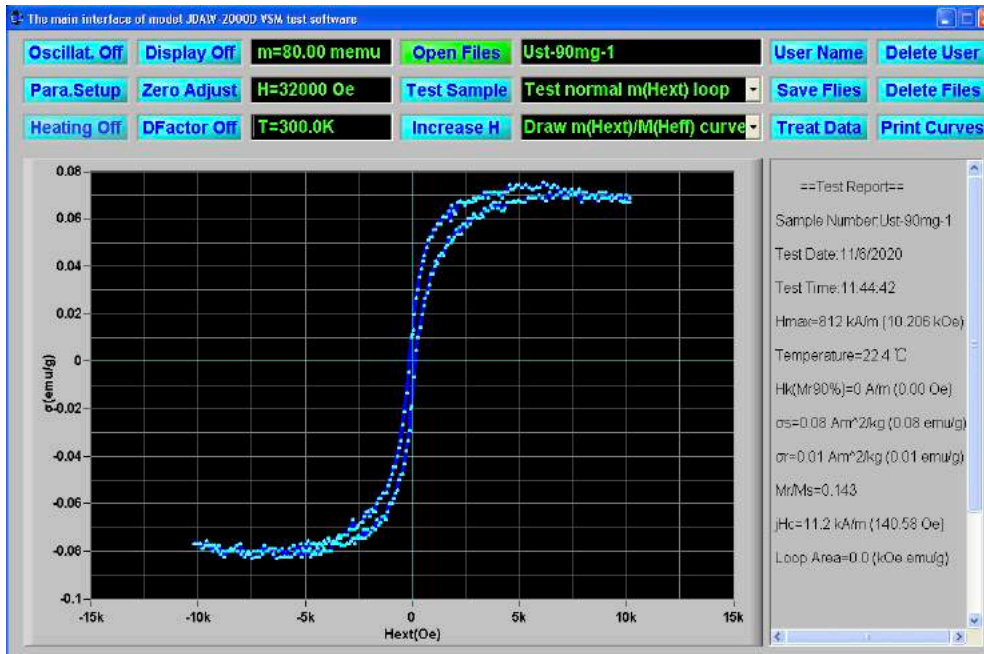


Figure 2.6: VSM result of the top part of the lead oxide plate sample.

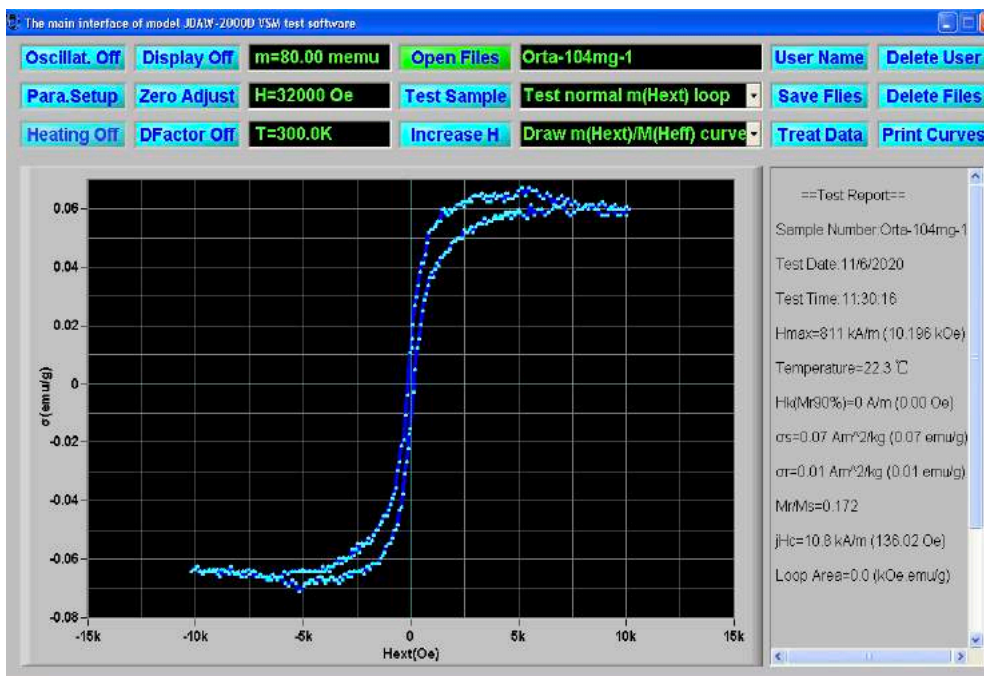


Figure 2.7: VSM result of the middle part of the lead oxide plate sample.

The existence of ferromagnetic impurities or domains at the atomic or microscopic level can be the cause of the surprise discovery of a ferromagnetic hysteresis curve in a sample that appears to be non-magnetic. When exposed to an external magnetic field during the VSM experiment, these locations might show induced magnetism. It emphasizes how crucial it is to fully characterize and comprehend the microstructure of the material before interpreting magnetic readings to prevent misunderstandings or incorrect conclusions.

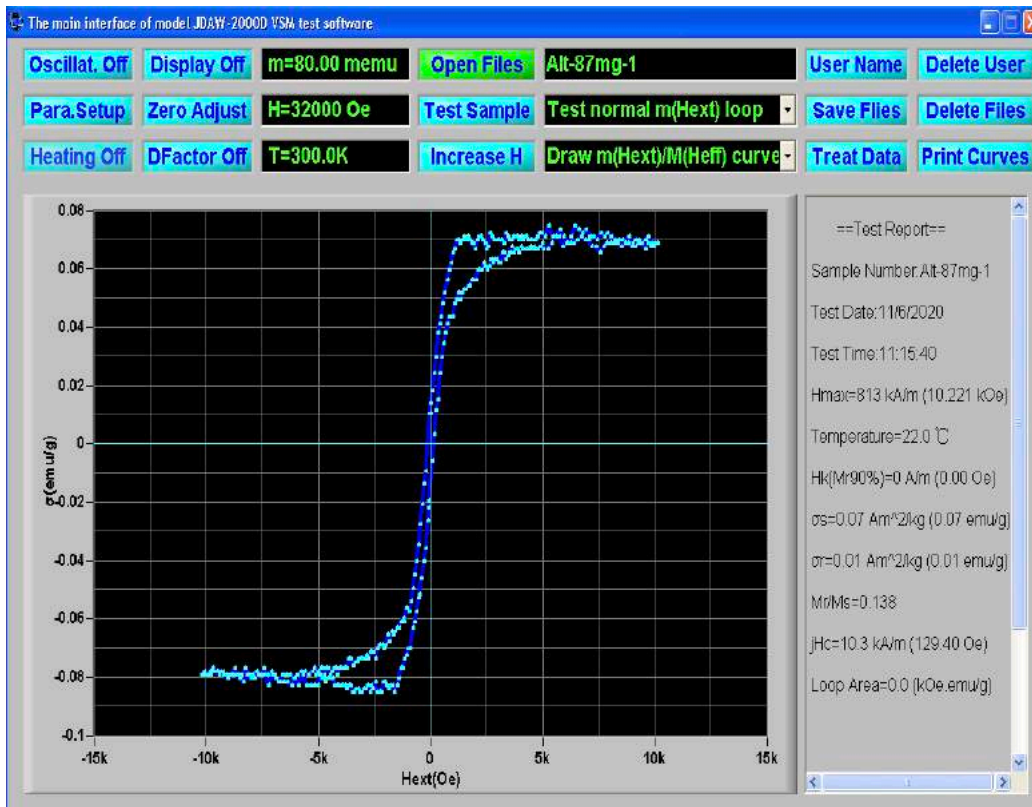


Figure 2.8: VSM result of the lower part of the lead oxide plate sample.

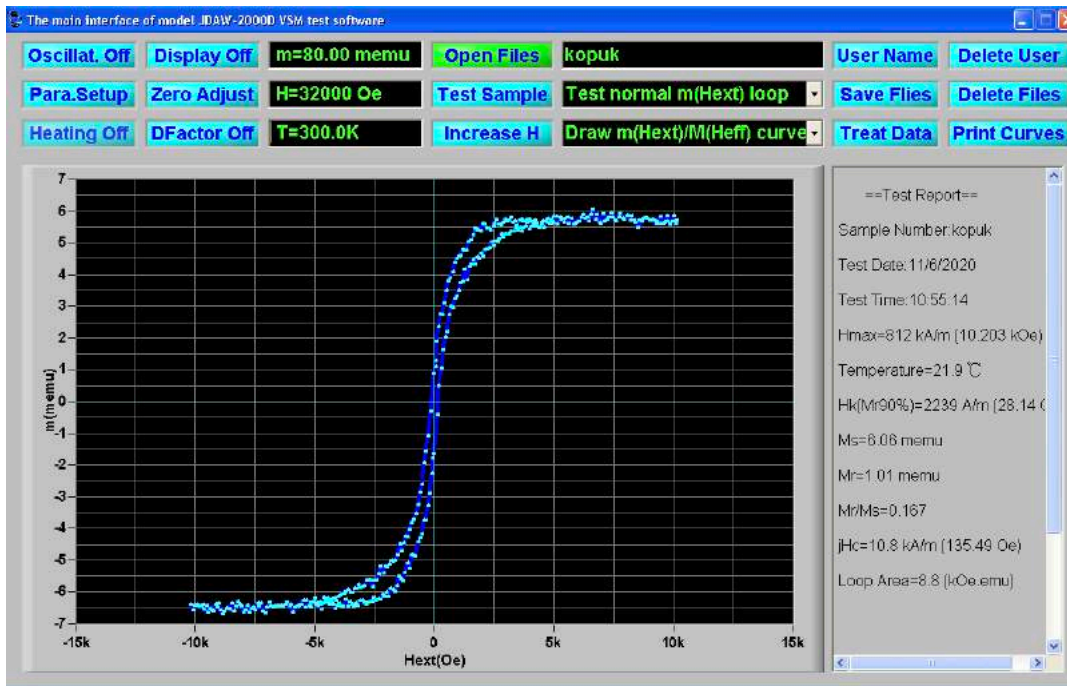


Figure 2.9: VSM result of the Styrofoam (no sample).

The Styrofoam sample is used for reference in the comparison of VSM results of lead oxide samples. As it can clearly be seen, there is no significant difference between the hysteresis plots.

2.2.5 The Particle Size Analysis

Particle size analysis plays a crucial role in characterizing radar-absorbing materials (RAMs) since it governs their efficacy in absorbing electromagnetic radiation across various frequencies [27]. The size of RAM particles directly impacts their capacity to absorb electromagnetic radiation. Notably, larger particle sizes lead to heightened reflectivity, as a greater portion of electromagnetic energy bounces back from the material's surface [28]. Conversely, smaller particle sizes increase electromagnetic radiation attenuation, resulting in enhanced absorption due to the larger material surface area [29].

Moreover, analyzing particle size offers valuable insights into the RAM's composition uniformity. A homogeneous distribution of particle sizes enhances the material's absorption capacity. Conversely, an uneven distribution may cause erratic absorption and electromagnetic radiation reflection [30].

The particle size analysis technique provides essential data on average size, distribution, and shape of particles in RAMs. This information proves critical for selecting appropriate RAMs tailored to specific applications, as particle size and shape significantly impact performance [31]. For example, materials composed of small, spherical particles excel at absorbing high frequencies but may underperform at lower frequencies due to limited wave path length. On the other hand, materials with irregularly shaped particles can absorb electromagnetic radiation across a wide frequency range, making them ideal for broadband applications.

This characterization technique additionally looks at the particle size of the Lead Oxide from the plates' top and bottom halves. All findings were made in Katip Çelebi University's Central Research Laboratory.

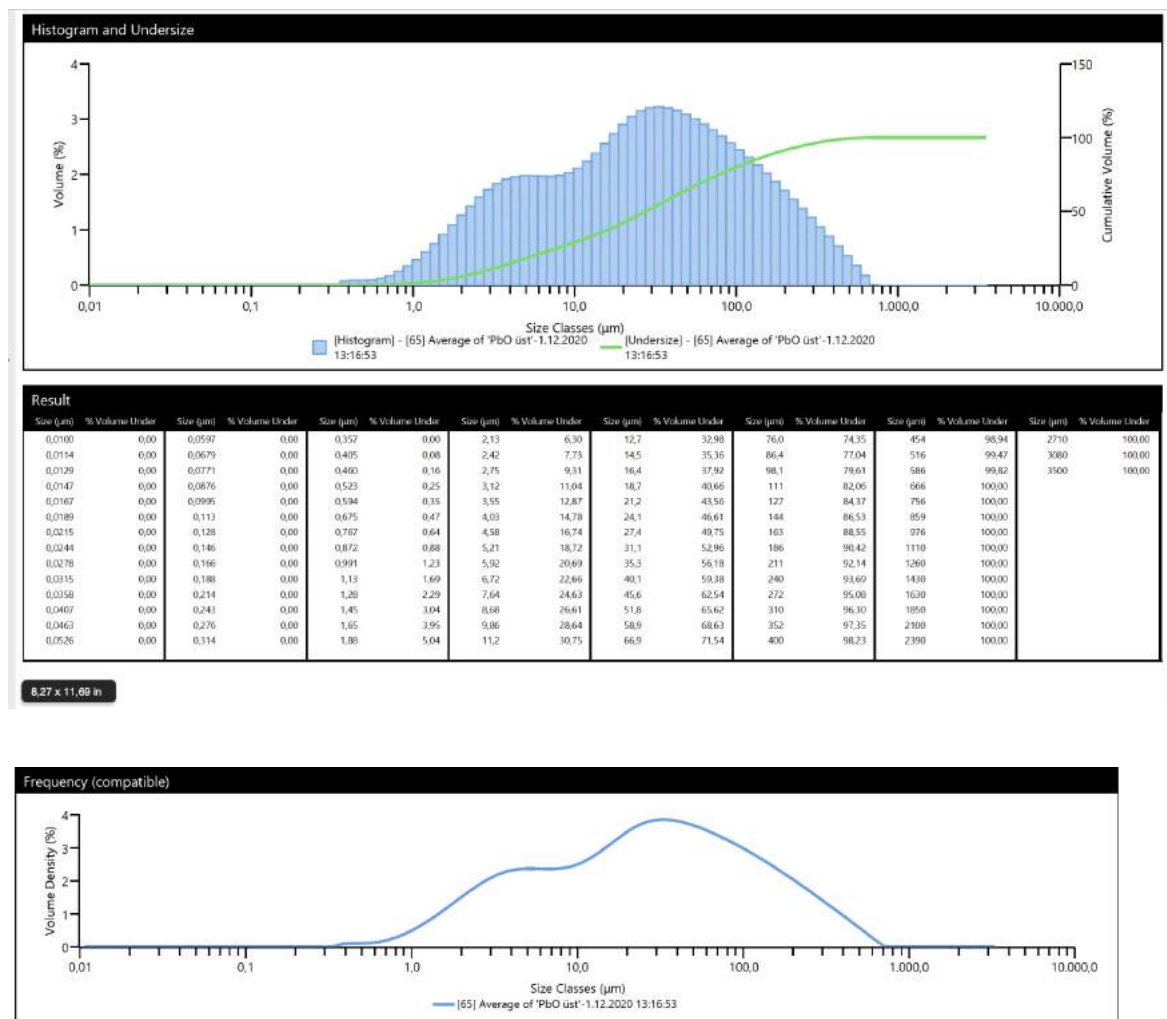
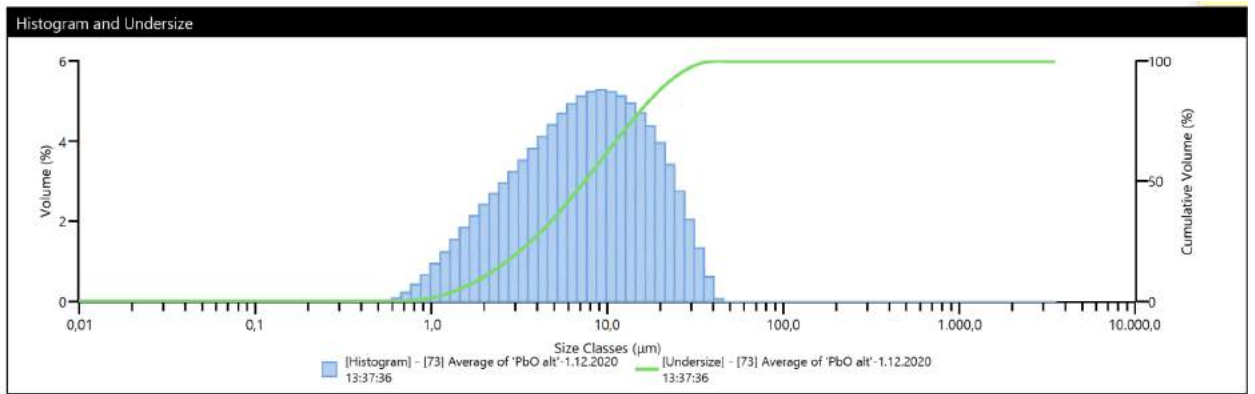


Figure 2.10: The particle size analysis result of the top part of the lead oxide plate sample.



Size (µm)	% Volume Under	Size (µm)	% Volume Under	Size (µm)	% Volume Under	Size (µm)	% Volume Under	Size (µm)	% Volume Under	Size (µm)	% Volume Under	Size (µm)	% Volume Under
0.0100	0.00	0.0557	0.00	0.357	0.00	2.13	11.51	12.7	71.80	76.0	100.00	454	100.00
0.0114	0.00	0.0679	0.00	0.405	0.00	2.42	14.20	14.5	76.75	86.4	100.00	516	100.00
0.0129	0.00	0.0771	0.00	0.460	0.00	2.75	17.16	16.4	81.45	98.1	100.00	586	100.00
0.0147	0.00	0.0876	0.00	0.523	0.00	3.12	20.39	18.7	85.83	111	100.00	666	100.00
0.0167	0.00	0.0995	0.00	0.594	0.00	3.55	23.90	21.2	89.78	127	100.00	756	100.00
0.0189	0.00	0.113	0.00	0.675	0.00	4.03	27.71	24.1	93.19	144	100.00	859	100.00
0.0215	0.00	0.128	0.00	0.767	0.31	4.58	31.82	27.4	95.94	163	100.00	976	100.00
0.0244	0.00	0.146	0.00	0.872	0.73	5.21	36.23	31.1	97.99	186	100.00	1110	100.00
0.0278	0.00	0.166	0.00	0.991	1.40	5.92	40.91	35.3	99.32	211	100.00	1260	100.00
0.0315	0.00	0.188	0.00	1.13	2.34	6.72	45.84	40.1	99.94	240	100.00	1430	100.00
0.0358	0.00	0.214	0.00	1.28	3.57	7.64	50.96	45.6	100.00	272	100.00	1630	100.00
0.0407	0.00	0.243	0.00	1.45	5.11	8.68	56.19	51.8	100.00	310	100.00	1850	100.00
0.0463	0.00	0.276	0.00	1.65	6.96	9.86	61.46	58.9	100.00	352	100.00	2100	100.00
0.0526	0.00	0.314	0.00	1.88	9.09	11.2	66.69	66.9	100.00	400	100.00	2390	100.00

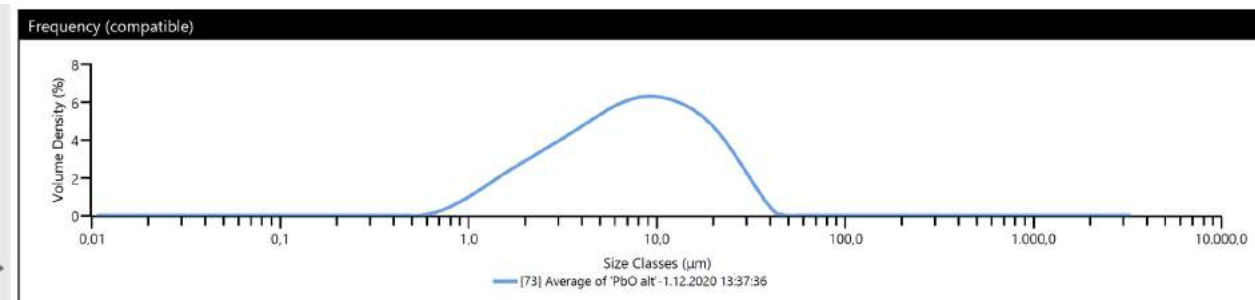


Figure 2.11: The particle size analysis result of the top part of the lead oxide plate sample.

2.2.6 X-Ray Diffraction

X-Ray Diffraction (XRD) analysis plays a crucial role in examining the intricate crystal structure and microstructure of materials. In the context of radar absorbing materials (RAMs), XRD emerges as a valuable tool, offering crucial insights into their composition, phase purity, crystal structure, and morphology. [32]

RAMs are ingeniously crafted to effectively absorb or disperse electromagnetic radiation within the radar frequency spectrum. They encompass a wide array of materials, such as metals, ceramics, polymers, and composites, each with distinct

morphologies and structures. The efficacy of RAMs depends on their capacity to attenuate incoming radiation, influenced by various factors like the absorbing material's type, size, crystal structure, and arrangement of elements. As a result, XRD proves instrumental in the analysis and optimization of RAM properties, including absorption coefficient and bandwidth, by characterizing their crystal structure and microstructure. [33]

XRD analysis also serves the purpose of identifying impurities and defects in RAMs, which play a crucial role in determining their overall performance. The presence of impurities can significantly alter the crystal structure and composition of the absorbing material, thereby impacting its electromagnetic characteristics. Likewise, defects, including dislocations, stacking faults, and vacancies, exert influences on the material's electronic and magnetic properties, ultimately reducing its absorption efficiency. Employing XRD, valuable insights into the nature and extent of defects within the material can be obtained, thereby facilitating the optimization of RAMs [34].

In addition, XRD finds utility in examining the effects of processing and fabrication techniques on the crystal structure and microstructure of RAMs. Processing methods such as ball milling, heat treatment, and mechanical deformation have the potential to influence the phase composition, grain size, and texture of the material, leading to consequential changes in its electromagnetic properties. By utilizing XRD to monitor these alterations, it becomes possible to fine-tune the processing conditions and achieve the desired material properties [35].

Lead oxide (PbO) is a chemical compound comprising lead and oxygen, adopting a cubic crystal structure, and classified under the space group Fm-3m. The X-ray diffraction (XRD) analysis of lead oxide reveals distinct peaks at specific angles (2θ), corresponding to atomic positions within the crystal structure.

The X-ray diffraction patterns of lead oxide can be readily accessed in various databases, such as the International Centre for Diffraction Data (ICDD) and the American Mineralogist Crystal Structure Database. These comprehensive repositories furnish vital information concerning peak positions, intensities, and other pertinent crystallographic data.

In addition, Figure 2.12 [36] presents a specific XRD pattern from the lead paste in a spent lead-acid battery prior to calcination, revealing the constituents of the spent lead paste, including PbSO_4 , PbO_2 , PbO , and other components.

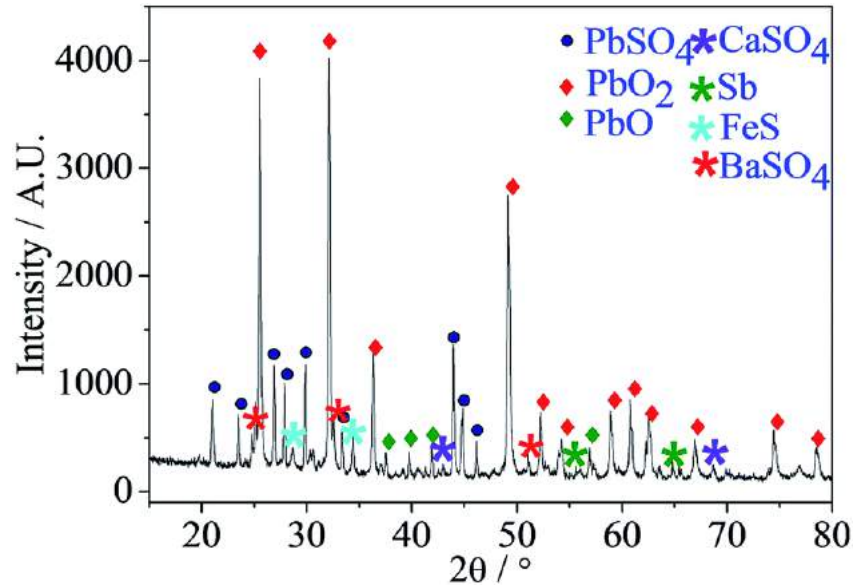
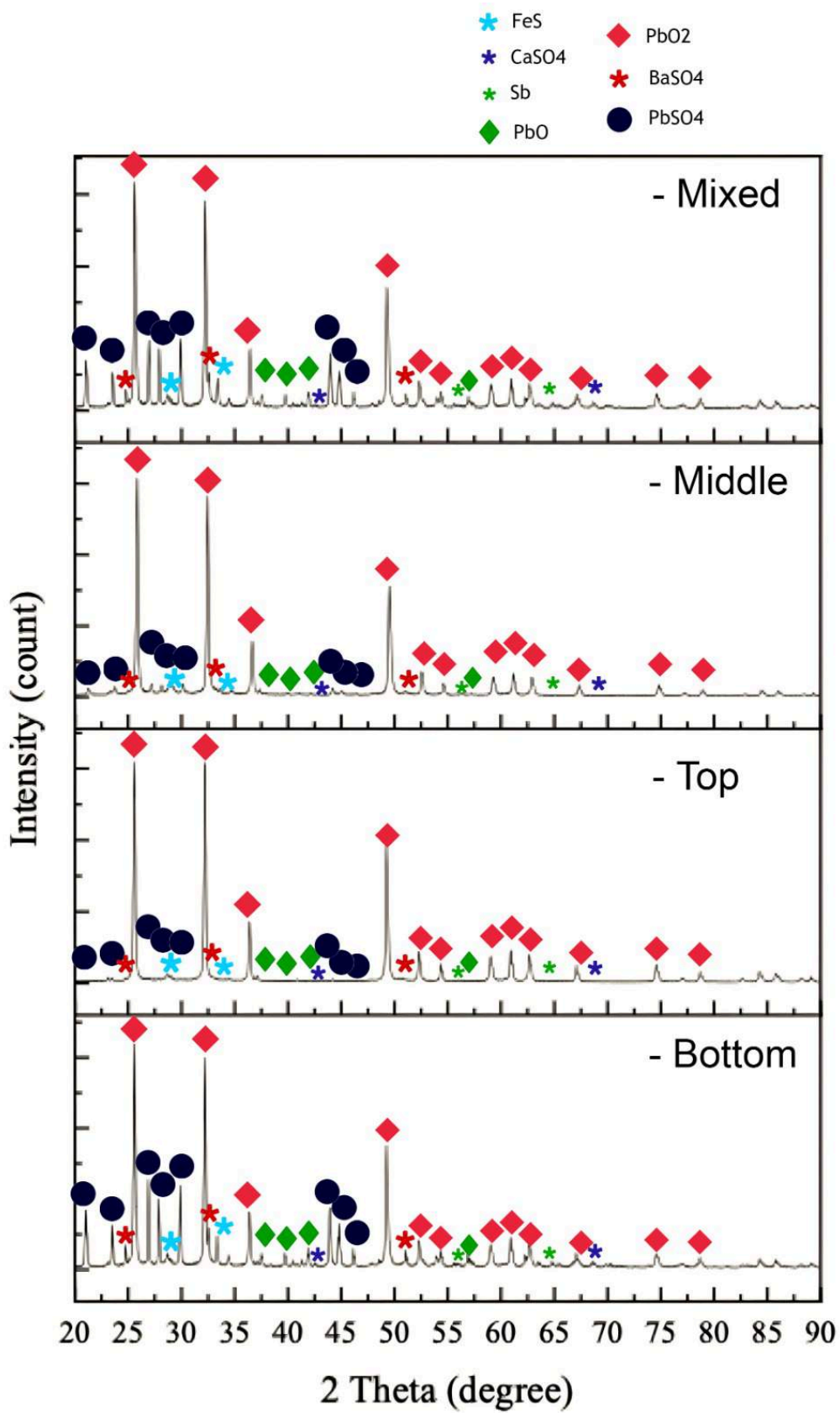


Figure 2.12 The XRD of the spent lead paste before calcination. [44]

The XRD results of the powder from recycled battery are obtained in the Laboratories of Material Science and Engineering Department in İzmir Katip Çelebi University. In Figure 13 PbO_2 peaks (25° , 33° and 49° - in all plots), PbSO_4 peaks (between 25° and 30° degrees- in mixed and bottom plots) and PbO peaks (between 50° and 60° degrees, 35° and 45° degrees - in mixed and bottom plots) can be clearly seen in combined XRD plots. The mixed powder contains powders from each region of the Lead Oxide plate.



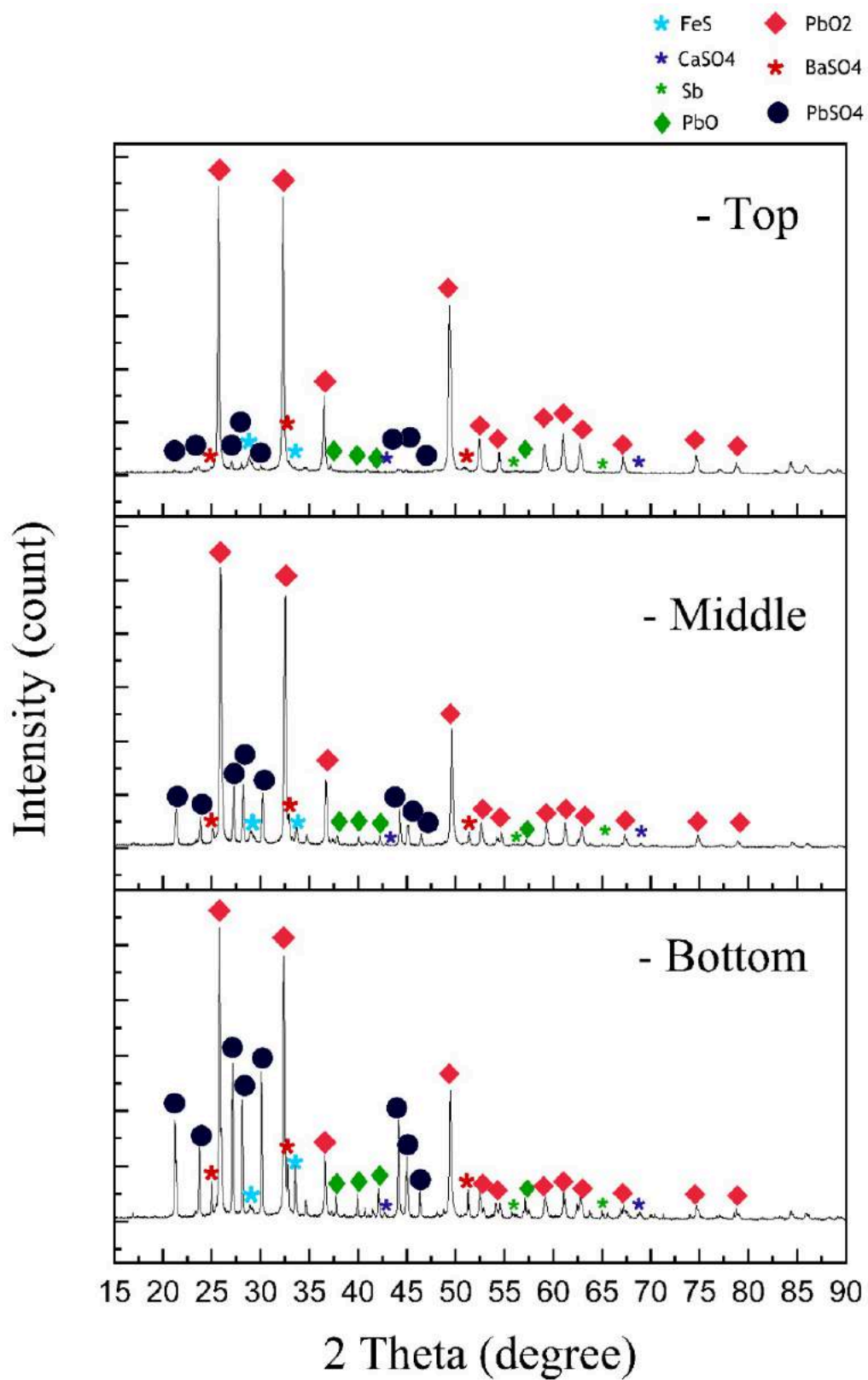


Figure 2.13 The XRD results of the non-grinded (above) and grinded (below) powder from the recycled battery.

The diffraction patterns show that extraction of lead oxide from the car battery was successful, and it normally and unsurprisingly contains sulfate. It is a natural result of the battery working mechanism. All peaks in the experimental XRD data results perfectly matched with the literature results.

Chapter 3

Materials and Methods

3.1 Filtering

The filtering process was made in İzmir Katip Çelebi University Sample Preparation Laboratory. Vibratory Sieve Shaker AS 200 Control (see Fig. 3.1, the photo is taken from the website of Retsch) was used. The lead oxide powder samples were filtered by 2 different sieves (130 micron and 75 micron). The 130-micron filtering process was 1 hour, and the 75-micron filtering process was 90 minutes. After the filtering process, 3 different sizes (above 135 microns, in between 135 and 75 microns, below 75 micron) were obtained.



Figure 3.1: Vibratory Sieve Shaker (Retsch)

3.2 The Design of RAMs

The size of the RAMs was formed with respect to the size of the waveguide of the network analyzer which has rectangle dimensions 1.0 cm and 2.2 cm. The single, double, and triple layered RAMs which were investigated in this thesis is shown in Fig.3.2.

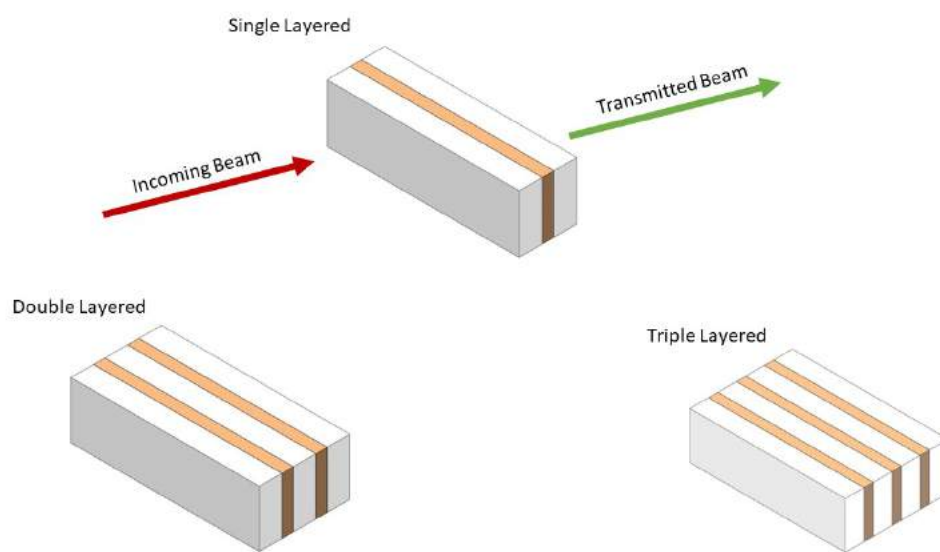


Figure 3.2: Single, double, and triple layered RAMs - combination of styrofoam (white colored) and lead oxide sample (brown colored).

3.2.1 Styrofoam

Expanded polystyrene, commonly known as Styrofoam, serves as a foam-based material ideal for its radar-absorbing capabilities in network analyzer measurements due to its remarkably low dielectric constant and loss tangent. These crucial properties render it exceptionally suitable for use in such measurements.

During network analyzer measurements, precision is paramount, necessitating a controlled environment that effectively mitigates reflections and other sources of potential error. Radar Absorbing Materials (RAMs) are skillfully employed to absorb

any remaining electromagnetic radiation not absorbed by the device under examination, effectively curtailing reflections and minimizing measurement errors.

The loss tangent provides insights into a material's dissipation of energy when subjected to an electric field, whereas the dielectric constant gauges its ability to retain electrical energy within such a field. Materials with low dielectric constants and loss tangents exhibit reduced energy absorption, thereby leading to diminished reflection and measurement errors in the context of network analyzer assessments.

Furthermore, the cost-effectiveness and widespread availability of Styrofoam render it a highly practical and viable option for use as a RAM in network analyzer measurements.

3.3 Vector Network Analyzer (VNA) Measurements

All measurements were made in EMUM (Elektronik Malzemeler Üretim ve Uygulama Merkezi) in Dokuz Eylül University. Vector Network Analyzer N5230C 300 kHz - 13.5 GHz by Agilent Technologies was used in between 8 and 12 GHz. The results for reflection loss S_{11} and transmission coefficient S_{21} (forward transmission (from port 1 to port 2)) in linear format were used.

Network analyzers typically utilize a straightforward format to display measurement results, employing linear representation to directly showcase the measured electrical signals. Although logarithmic scales like the decibel (dB) scale hold certain advantages, linear scales are often favored for specific measurement scenarios.

Advantages of using linear results:

1. Direct representation of signals: Linear measurements offer a straightforward portrayal of the actual electrical signals under examination, proving invaluable for diverse analyses such as signal processing, circuit design, and system optimization.
2. Accurate depiction of small signals: Linear scales excel at accurately representing minute signals that might prove elusive on a logarithmic scale. This

capability is particularly crucial for gauging low-level signals or detecting subtle changes in signal amplitude.

3. Ease of interpretation: Linear scales are generally easier to interpret, especially for individuals unfamiliar with the decibel scale. They enable straightforward comparisons of signal amplitudes and facilitate visualizing changes in signal levels.
4. Enhanced precision: Linear scales provide heightened accuracy for specific measurements, such as reflection coefficients or voltage standing wave ratio (VSWR), often applied in antenna and microwave measurements.

The merits of logarithmic scales include representing large dynamic ranges and ratios, but linear scales are often preferred due to their direct signal representation, accuracy for small signals, ease of interpretation, and better precision in certain measurement scenarios.



Figure 3.3: Vector Network Analyzer N5230C 300 kHz - 13.5 GHz by Agilent Technologies was used in between 8 and 12 GHz.

The frequency range between 8 to 12 GHz finds widespread application in radar absorbing materials (RAMs) measurements using network analyzers. Many materials exhibit high absorption properties within this X-band frequency range, which is also

commonly used in radar and communication systems like weather radar, military radar, and airport radar systems. Additionally, satellite communication and microwave communication systems frequently rely on this frequency range.

Selecting a frequency range with high absorption properties is crucial for RAMs measurements to minimize reflections and measurement errors. The 8-12 GHz frequency range is well-established and standardized, facilitating data comparison and sharing across different research groups and industries, making it a preferred choice for various measurements and applications.

Chapter 4

Results and Discussions

4.1 VNA Results

In the first phase in my research, grinded Lead oxide powder was not categorized in terms of size. The broad range of particle size was mixed in the powder as seen in Particle size and SEM characterization methods. The results for reflection loss S_{11} and transmission coefficient S_{21} (forward transmission (from port 1 to port 2)) in linear format were obtained from Vector Network Analyzer N5230C. In order to confine the Lead oxide powder, the simple paper was used. The rectangular shape of paper was prepared with respect to the size of the waveguide of the Network Analyzer. After distributing the powder uniformly inside the rectangular paper box, the adhesive tape was used to prevent the box from opening accidentally.

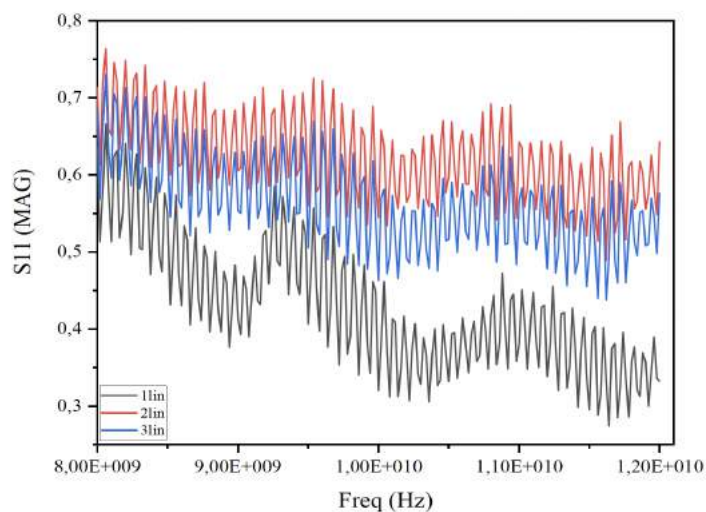


Figure 4.1: S_{11} for the non-grinded lead oxide powder inside a paper matchbox. Black 50 mg, Red 100 mg, Blue 150 mg.

Figure 4.1 shows reflection loss in between 8 and 12 GHz for different amounts of lead oxide powder which contains mixed particle size (unfiltered).

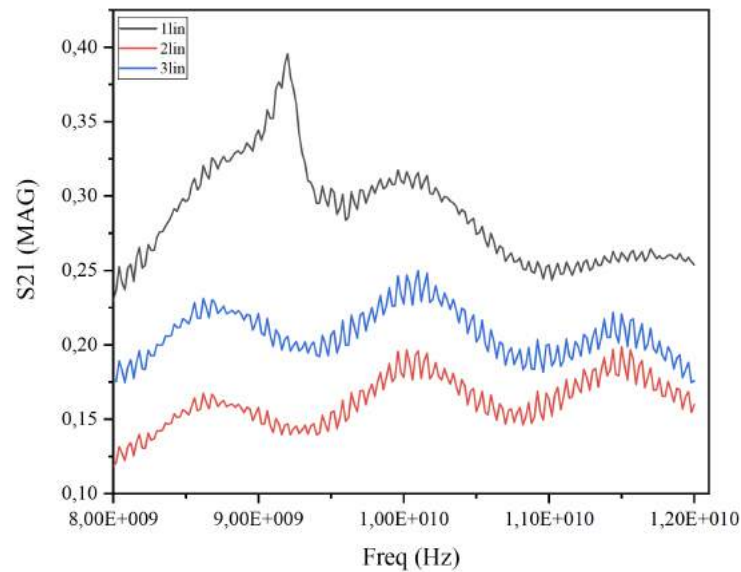


Figure 4.2: S_{21} for the non-grinded lead oxide powder inside a paper matchbox (see above). Black 50 mg, Red 100 mg, Blue 150 mg.

Figure 4.2 shows transmission coefficient in between 8 and 12 GHz for different amounts of lead oxide powder which contains mixed particle size (unfiltered). As seen from the diagram, the paper matchbox with the least lead oxide powder has got low reflection and high transmission rates around 10 GHz.

In the second phase of the experiment, the paper was replaced by styrofoam. Then the same setup was repeated with different amounts of lead oxide powder. As a reference sample, the empty styrofoam was also used.

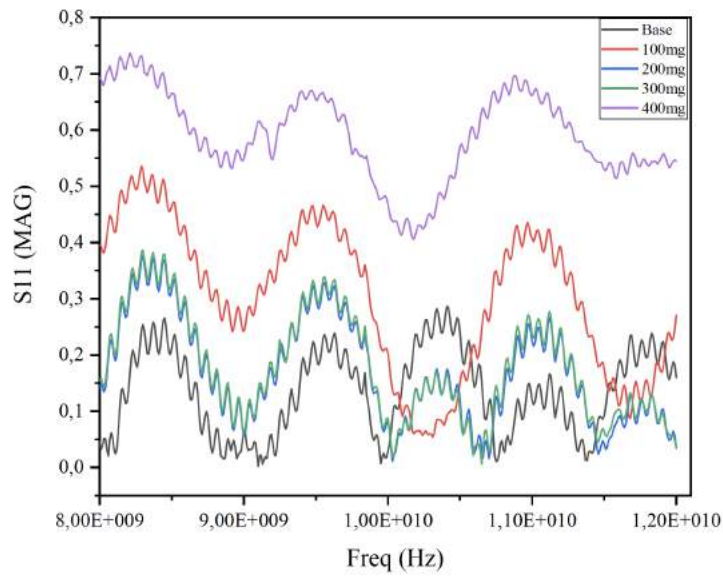


Figure 4.3: S_{11} for empty and different amounts of the non - grinded lead oxide powder inside a single styrofoam.

The samples with 400 mg and 100 mg lead oxide show the lowest reflection around 10 GHz.

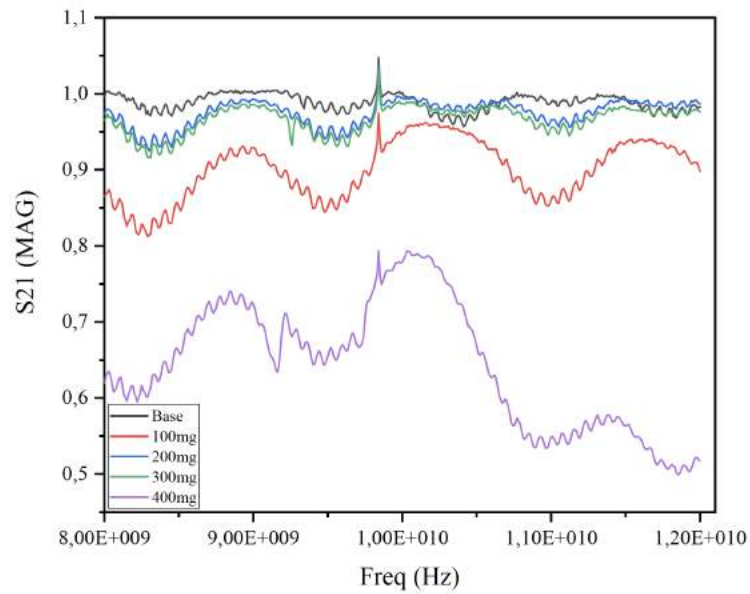


Figure 4.4: S_{21} for empty and different amounts of the non -grinded lead oxide powder inside a single Styrofoam.

Higher transmission rates are seen in Fig. 4.4. If a wave is not transmitted, it should have only 3 other ways - scattering, reflecting, and absorbing.

In the next step, filtered lead oxide powder was analyzed by VNA. Three different size ranges were used to design RAM samples with styrofoam: Smaller than 75 micron - between 75 micron and 130 micron - greater than 130 microns.

The different variations of size and powder parts of the plates (the samples taken from the top, the bottom, and the intermediate parts) were analyzed in VNA. Figure 4.5 below shows S_{11} for the same (100 mg) amount of the grinded lead oxide powder inside a single Styrofoam with different particle size (smaller than 75 micron and sample taken from the bottom part of the plate - black, between 75 micron and 130 micron - red, greater than 130 micron - blue).

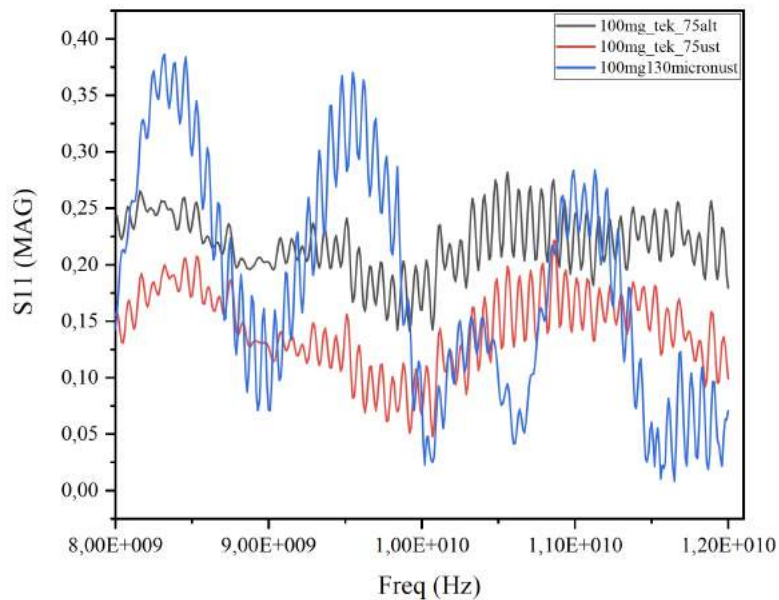


Figure 4.5: S_{11} for the same (100 mg) amount of the grinded lead oxide powder inside a single Styrofoam with different particle size: the smaller than 75 micron and the sample taken from the bottom part of the plate - black, between 75 micron and 130 micron - red (the sample taken from the top part of the plate), greater than 130 micron - blue (the sample taken from the top part of the plate).

The transmission coefficient for the same samples for the same frequency range is shown below.

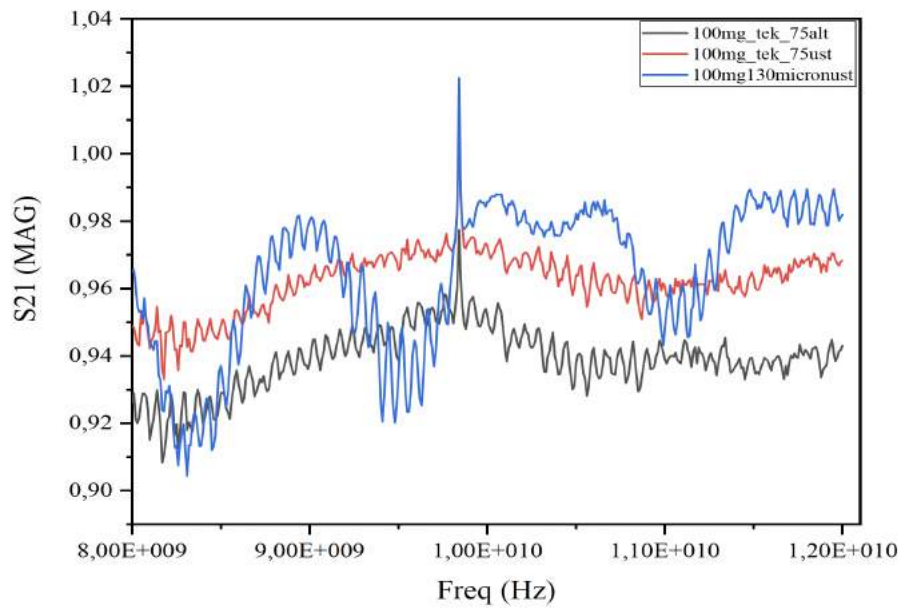


Figure 4.6: S_{21} for the same (100 mg) amount of the grinded lead oxide powder inside a single Styrofoam with different particle size: the smaller than 75 micron and the sample taken from the bottom part of the plate - black, between 75 micron and 130 micron - red (the sample taken from the top part of the plate), greater than 130 micron - blue (the sample taken from the top part of the plate).

Furthermore, the single and the double layered samples that contain equal total amounts of lead oxide whose size is bigger than 130 microns were also analyzed. The double layered RAM had layers which contain 50 mg that give 100 mg in total. It is compared with the RAM which contains 100 mg in 1 layer.

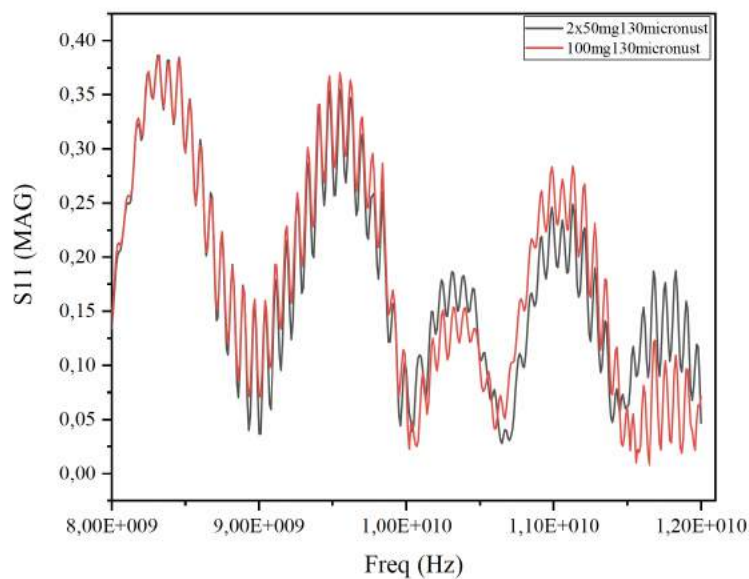


Figure 4.7: S_{11} for the Single and double layered lead oxide (the particle size bigger than 130 micron).

The similarity in the diagram is absolute and quite clear. The same procedure and logic were applied in the next step. This time 3 layered (triple) RAM against 1 layered RAM that contain the same amount of lead oxide in total were analyzed for the same spectrum (8 - 12 GHz). The particle size for both RAM samples was held constant (bigger than 130 micron). The results for reflection and transmission coefficients can be seen below:

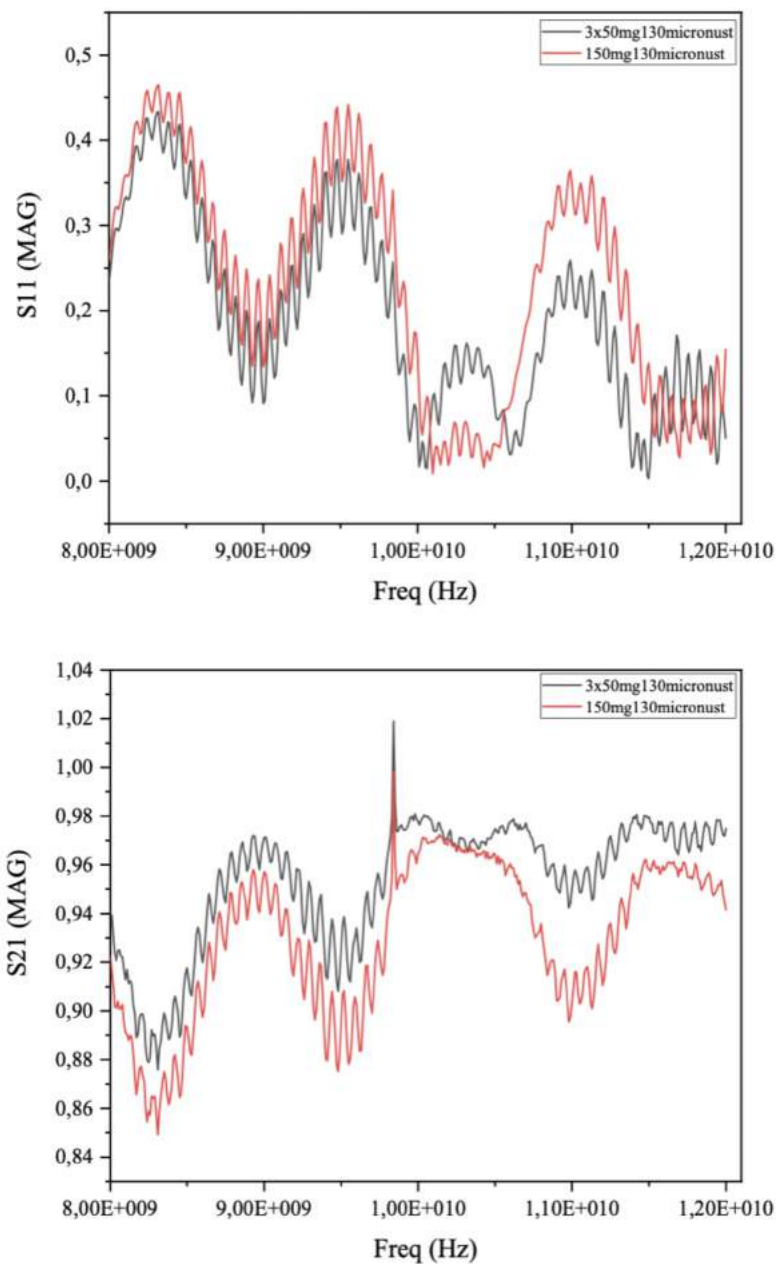


Figure 4.8: S_{11} and S_{21} for the single and triple layered Styrofoam RAM samples which contain the same total amount of lead oxide (the particle size is bigger than 130 micron).

The double layered (50 mg + 50 mg and 150 mg + 150 mg) and the triple layered (50 mg + 50 mg + 50 mg) Styrofoam RAM samples were also compared as shown below:

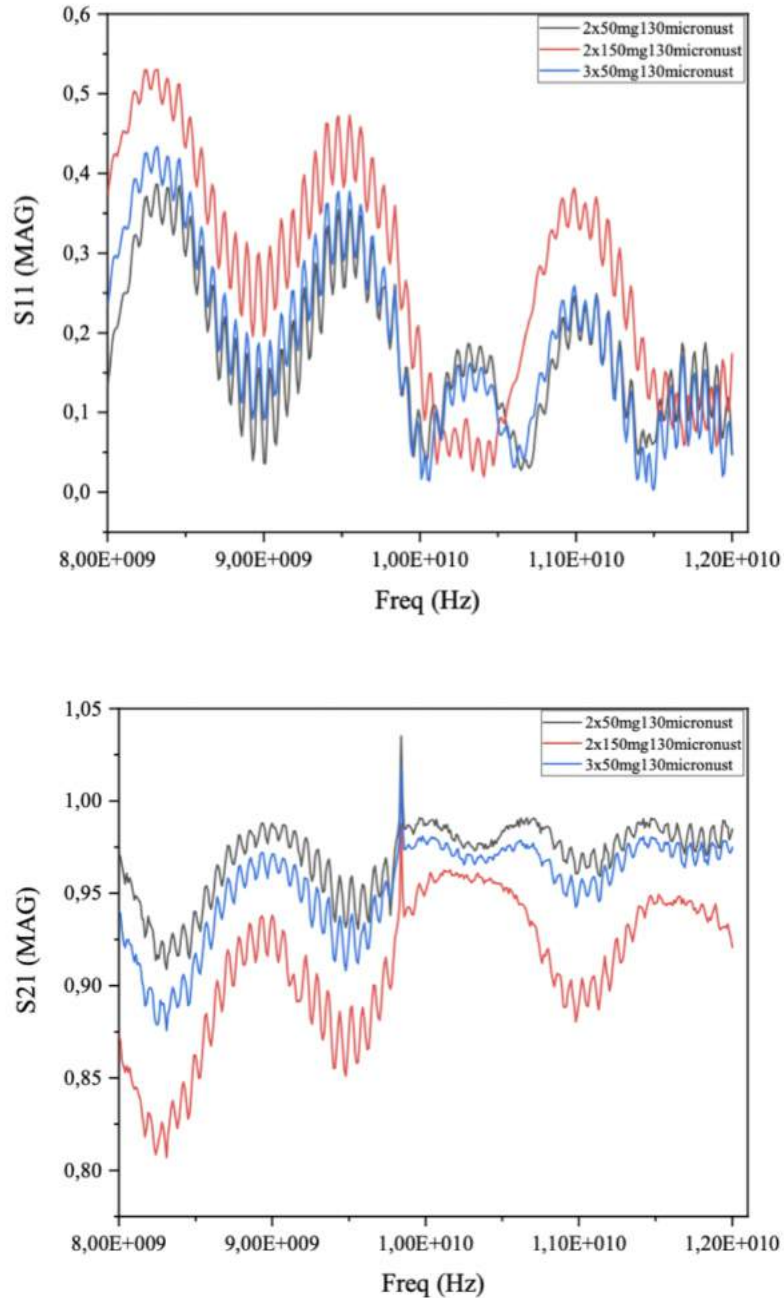


Figure 4.9: S_{11} and S_{21} for the double and triple layered Styrofoam RAM samples which contain different amounts of lead oxide (the particle size is bigger than 130 micron).

The double layered RAMs with different particle size (below and above 75 micron) were also analyzed. S_{11} and S_{21} for the two RAMS with different sizes can be seen in Figure 26.

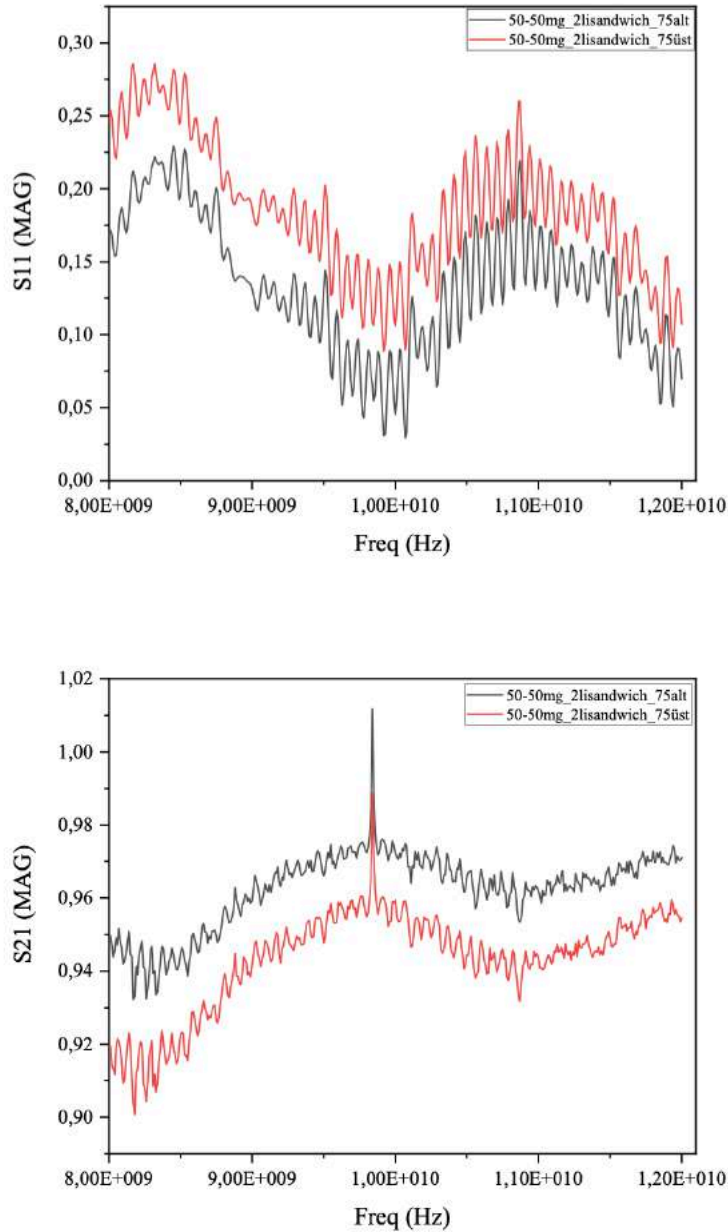


Figure 4.10: S_{11} and S_{21} for the double layered RAMs with different particle sizes (below and above 75 micron).

S_{11} and S_{21} can be seen for different amounts of lead oxide in a single layered RAM for the same particle size (below 75 micron) in Figure 4.11.

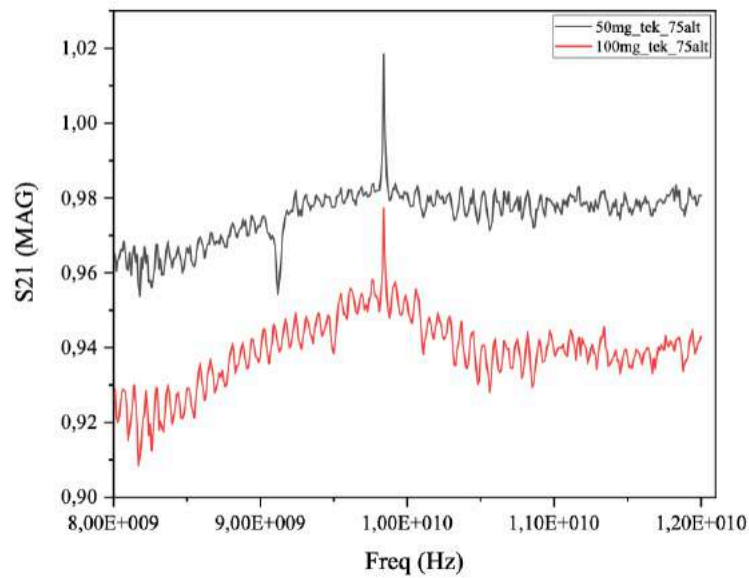
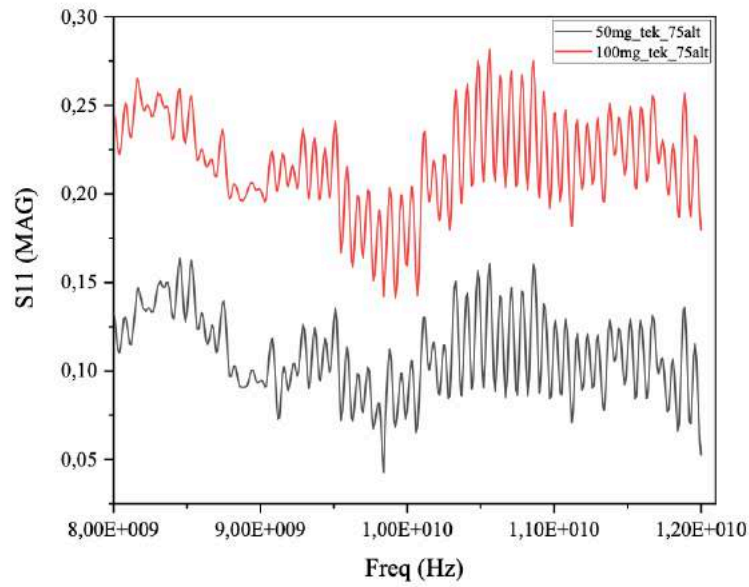


Figure 4.11: S_{11} and S_{21} can be seen for different amounts of lead oxide in a single layered RAM for the same particle size (below 75 micron)

The same procedure was also applied for the particle size greater than 75 microns. S_{11} and S_{21} for the single layer RAMS with different amounts of lead oxide in the same particle size (above 75 micron) is shown in Figure 4.12.

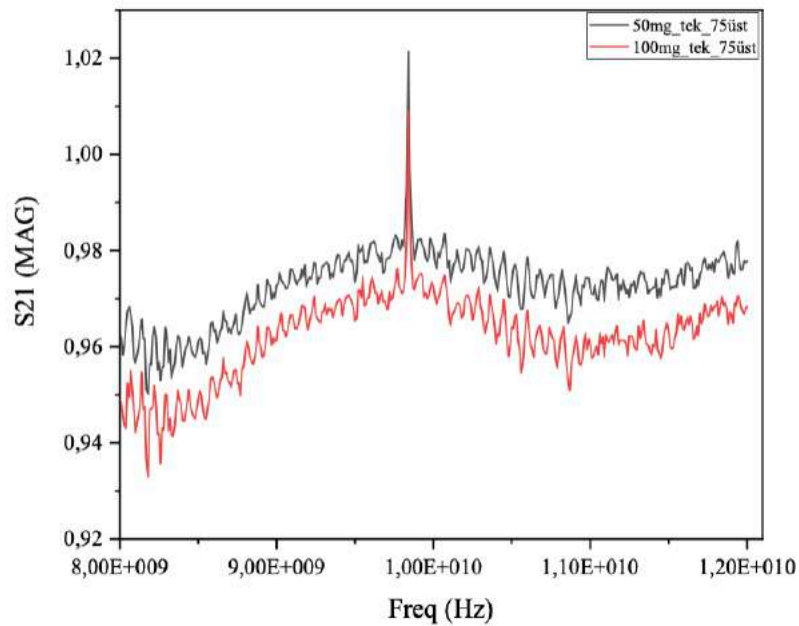
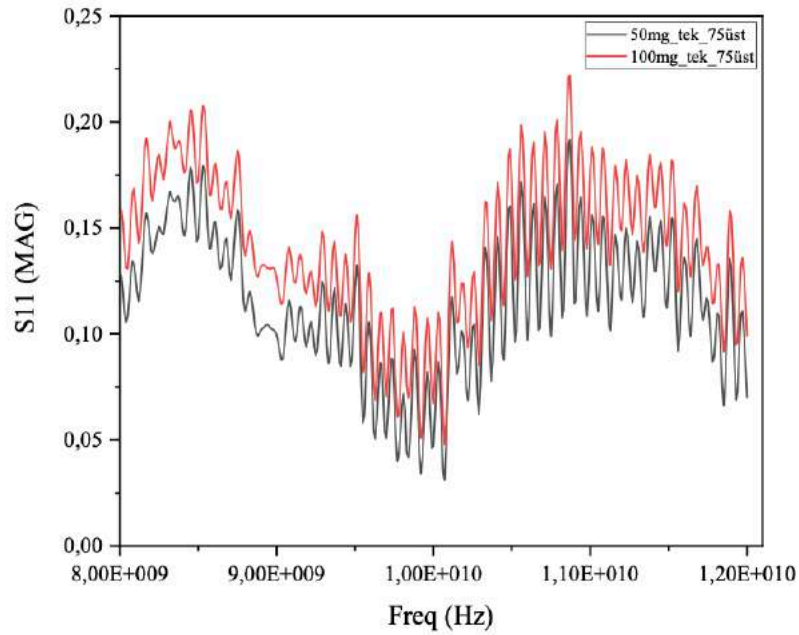


Figure 4.12: S_{11} and S_{21} for the single layer RAMS with different amounts of lead oxide in the same particle size (above 75 micron).

The steps which were taken until the last phase can be summarized as below:

- 1- Recycled lead oxide powder was categorized into 3 parts (top - middle - bottom) with respect to division of lead oxide battery plate.
- 2- The bottom part which contains more sulfates gave the least reflection, so we continued with this part.

3- After characterization methods (SEM, Particle Size, XRD ...), the powder was ground for 20 seconds inside the grinder which has stainless steel blades and works in 50 Hz (230 V, 110 W).

4- After the grinding, the size classification was made by filtering. Two sieves were used for dry filtering (135 micron and 75 micron). Size classified powders were used in single, double, and triple layered RAMs. The VNA results were taken for different particle sizes and the different sandwich layers of RAMs. Lead oxide gave high reflection loss between 8 - 12 GHz frequency interval.

As a next step, the smaller particle size was used. When the particle size becomes smaller, the radar absorbing properties can undergo changes. These changes can be summarized as shown below.

Enhanced Absorption:

Augmented Surface Area: Reducing particle sizes typically leads to a higher surface area within a given volume. This amplified surface area creates greater chances for electromagnetic wave absorption and scattering, consequently bolstering radar absorption [37].

Numerous Scattering: Diminishing particle sizes allows for multiple scattering events, prolonging the interaction time between incident radar waves and particles. This prolonged interaction enhances absorption capabilities [38].

Frequency-Dependent Absorption:

Resonant absorption concerning size: Under certain circumstances, resonance absorption can occur when the particle size aligns with the wavelength of incident radar waves. Such size-resonant absorption significantly enhances radar absorption at specific frequencies [39].

Scattering dependent on size: smaller particles demonstrate more efficient scattering of shorter wavelengths, making their radar wave scattering capability influenced by their size relative to the wavelength of the incident waves [40].

Absorption Bandwidth:

Wide-ranging broadband absorption: smaller particles of diverse sizes and shapes can exhibit characteristics of broadband radar absorption. The presence of particles with varying sizes contributes to absorption across a broader spectrum of radar frequencies [41].

Selective narrowband absorption: In specific cases, radar absorption properties may display a narrowband behavior due to size or shape effects, resulting in selective absorption at particular frequencies [42].

Filtering Procedure: A 25-micron sieve was employed during the filtering process, rendering the optical properties clear. The lead oxide powder's color exhibited a reddish hue, as depicted in Figure 29 below.



Figure 4.13: Comparison of lead oxide powder. The smaller particle size (below 25 micron) looks much more reddish (left) and the greater particle size (above 135 micron) looks completely brown.

The optical properties of lead oxide, particularly lead (II) oxide or PbO , exhibit an intriguing characteristic wherein its color tends to shift towards a more reddish hue as the particle size diminishes. This fascinating phenomenon, termed the "particle size effect," is closely linked to light scattering and absorption mechanisms.

In the case of bulk lead oxide, the larger particles have the ability to scatter light over a broader spectrum, resulting in a yellowish appearance. This scattering phenomenon arises due to interactions between incident light and the lead oxide particles, whose sizes can be comparable to or even larger than the wavelength of visible light [43].

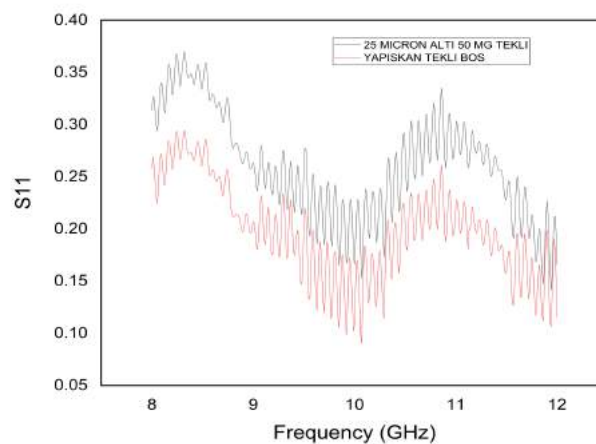
However, when it comes to lead oxide nanoparticles, the reduction in particle size leads to a substantial increase in the surface-to-volume ratio. This has a direct impact on the electronic structure and energy levels of the material. The changes in the electronic structure cause the selective absorption of specific wavelengths of light, particularly

shorter wavelengths in the blue region of the visible spectrum. As a consequence, the complementary color, which is the color opposite to the absorbed wavelengths, becomes more pronounced, giving rise to a reddish appearance [44].

The observed reddish color in smaller lead oxide particles, therefore, arises from both reduced light scattering across a broad spectrum and the selective absorption of shorter wavelengths, leading to a shift towards the red end of the visible spectrum.

The VNA results show that the Lead Oxide powder contains particles with a size below 25 microns, as depicted in the figures below:

The first RAM sample which contains 50 mg lead oxide powder with particle size below 25 micron was compared with our reference, adhesive tape. S_{11} and S_{21} for the single layer RAM with the same amount of lead oxide in the same particle size (below 25 micron) versus sellotape (adhesive tape) can be seen in Figure 4.14.



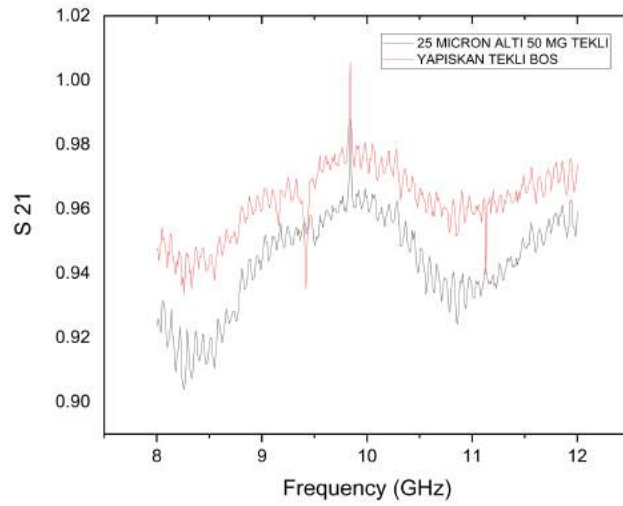
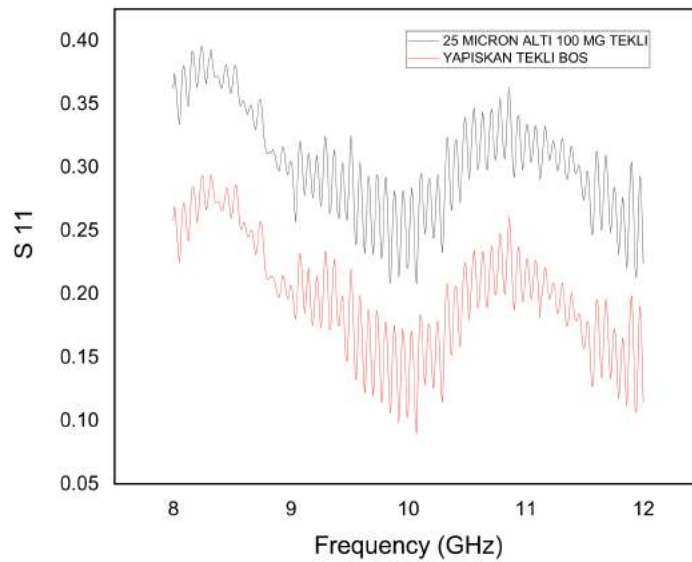


Figure 4.14: S_{11} and S_{21} for the single layer RAM with the same amount of lead oxide in the same particle size (below 25 micron) versus sellotape (adhesive tape).

The results are impressive, and it can be clearly seen that the smaller particle size resulted in greater reflection loss. In the second step, the amount of lead oxide powder was increased and compared with adhesive tape again.



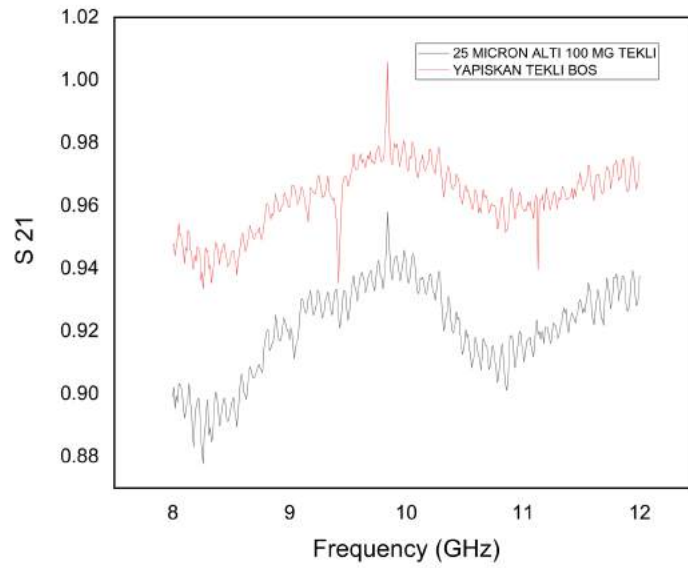
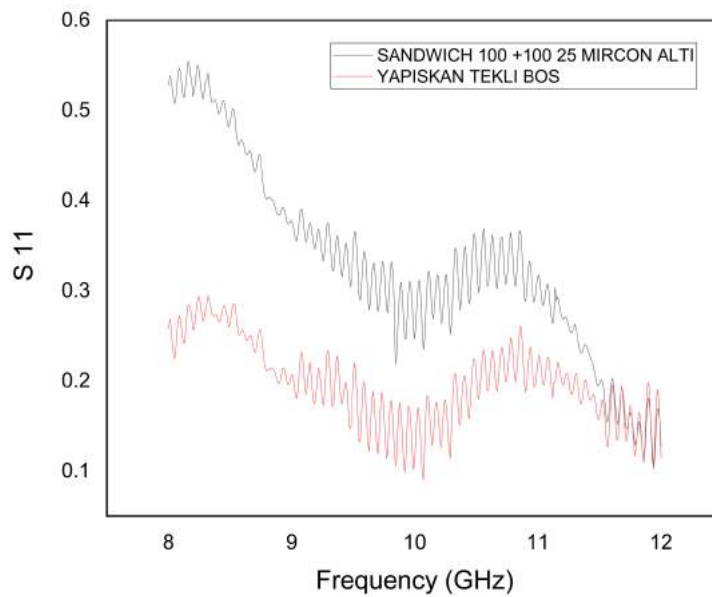


Figure 4.15: S_{11} and S_{21} for the single layer RAM which contains 100 mg lead oxide.

The double layered (sandwich) and double amount (100 mg + 100 mg) of lead oxide RAM samples were also analyzed and compared with adhesive tape as seen in Figure 4.16.



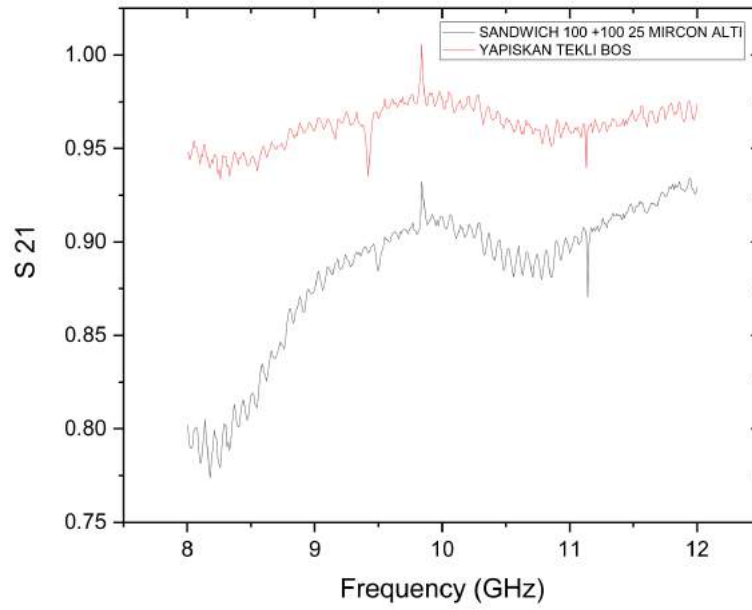
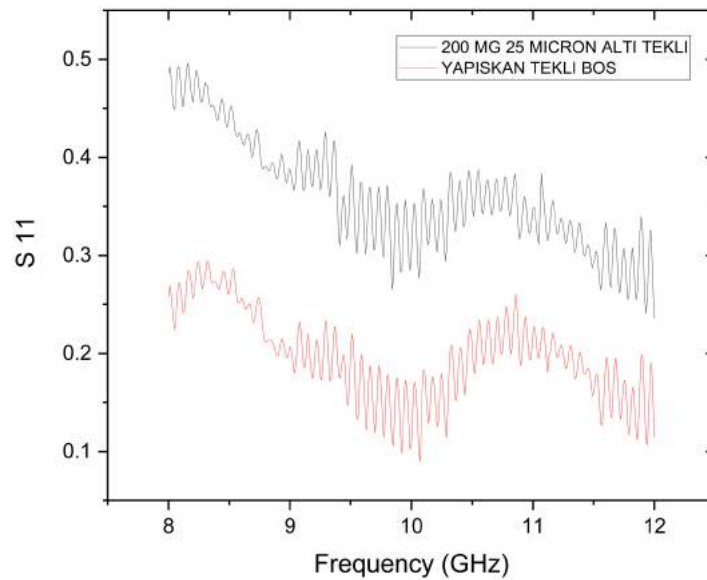


Figure 4.16: S_{11} and S_{21} for the double layered RAM which contains 200 mg lead oxide in total.

As a final step, the total amount (200 mg) was held constant, and the design was changed to single layer.



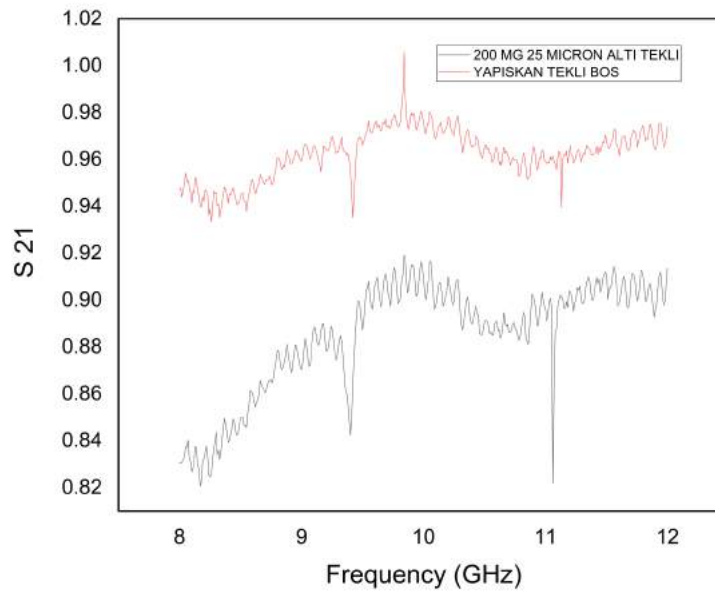


Figure 4.17: S_{11} and S_{21} for the single layer RAM which contains 200 mg lead oxide in total.

Evidently, various alterations, such as diverse particle sizes and quantities of lead oxide, as well as combinations of different RAMs' layers and lead oxide from distinct plate sections, yielded remarkably high transmission coefficients.

Radar Absorbing Materials (RAMs) serve the purpose of absorbing and attenuating electromagnetic waves, including radar signals. It's crucial for RAMs to maintain low transmission rates of radar signals to ensure their efficacy.

RAMs find application in reducing the radar cross-section (RCS) of objects, effectively concealing them from radar detection. When a radar signal encounters a RAM, the material absorbs and dissipates the signal energy, diminishing the reflected energy back to the radar receiver. This reduces the object's RCS, enhancing its stealthiness.

A RAM that allows high transmission rates of radar signals implies inadequate absorption and attenuation of signal energy, rendering it ineffective in reducing an object's RCS. The high transmission rates permit more radar energy to penetrate the RAM, leading to increased RCS, making the object more susceptible to radar detection. [45]

In the quest to lower the transmission rate S_{21} , Carbon-based materials have emerged as valuable candidates due to their exceptional electrical and magnetic properties. Notably,

materials like graphite and coal have been employed as effective absorbers. One crucial attribute of these materials is their high electrical conductivity, particularly evident in substances like graphene [46]. By incorporating such Carbon-based materials into radar absorbing materials, they exhibit the capability to efficiently dissipate incident electromagnetic energy by transforming it into heat. This energy conversion significantly reduces the amount of transmitted energy, leading to a decrease in radar wave transmission.

The absorbing and scattering properties of Carbon-based materials are equally remarkable, extending to electromagnetic waves, including radar waves [47]. The interaction between radar waves and Carbon-based materials, such as graphene or coal particles, brings about absorption and scattering phenomena. As a result, the energy of radar waves is diminished, preventing their seamless transmission through the material.

Moreover, Carbon-based materials boast the capacity to reflect radar waves [48]. Consequently, when radar waves strike the surface of a Carbon-based material, a portion of these waves is reflected rather than transmitted. This reflective capability further contributes to reduced radar wave transmission, effectively enhancing the material's radar signal absorption and attenuation efficiency.

Various carbon-based materials may display distinct levels of radar absorption and transmission reduction. As a result, two types of carbon-based materials, coal, and graphite, were employed in the study.

Graphite emerges as a robust microwave-absorbing material, showcasing exceptional capability in withstanding elevated temperatures while delivering high heating rates. [49]

Traditionally, radar-absorbing materials (RAMs) adopt a sheet-like structure comprising insulating/conducting polymers, such as rubber, combined with magnetic or dielectric loss materials like mixtures of carbon black and graphite or short carbon fibers. [50] These materials exhibit the capacity to absorb a substantial fraction (20–26%) of electromagnetic energy within a mere range of millimeters to centimeters of thickness. [51]

Sample Preparation

Lead oxide - carbon absorber (graphite or coal) containing epoxy RAM samples were prepared in following steps:

- Preparation of epoxy with 3 % stiffener (Figure 4.18)
- Preparation of mixture (PbO_2 & graphite or coal)
- 900 mg (100 % of the sample) and 9 mg is 1 %
- Graphite and coal powders are prepared until maximum value 3 % (Figure 4.19)
- The thickness of the sample should not exceed 2 mm for the best VNA results
- After mixing properly, the waveguide molds are filled by the epoxy mixture (Figure 36)



Figure 4.18: The preparation of epoxy with 3 % stiffener



Figure 4.19: Graphite and coal powders are prepared until maximum value 3 % inside the mixture of epoxy.



Figure 4.20: The waveguide molds are filled by the epoxy mixture.

The graphite source was 8B pencil lead. An 8B pencil has 90% graphite, 4% clay, and 5% wax. The clay content should be decreasing as the B grade increases. [52]

VNA Results

- 2 different sizes and different amounts of PbO_2 (above 75 micron and below 25 micron) were used.
- The coal and graphite powder were used as carbon sources.
- The multi-plots of constant amounts of PbO_2 versus varying amounts of coal and varying amounts of graphite were compared.

- The multi-plots of varying amounts of PbO₂ versus constant amounts of coal and graphite were compared.

- The multi-plots of varying size of PbO₂ versus constant amounts of coal and graphite were compared.

- Empty epoxy and 2 different sizes of PbO₂ (without carbon source - No graphite or coal) were used as control samples (reference point) in the plots.

Constant Amount of Graphite with Changing Amount of PbO₂ (below 25 micron)

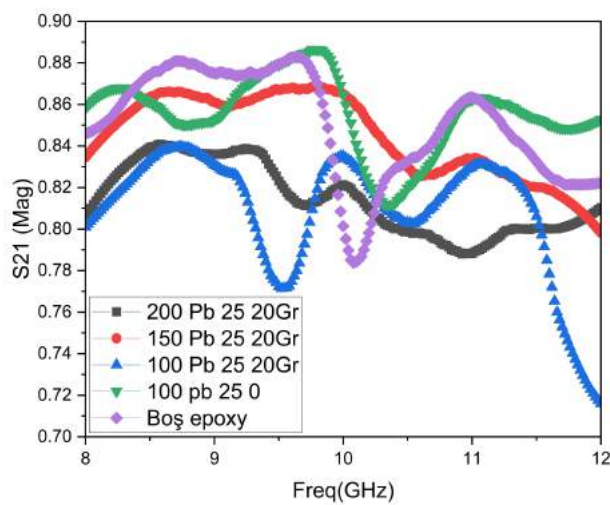
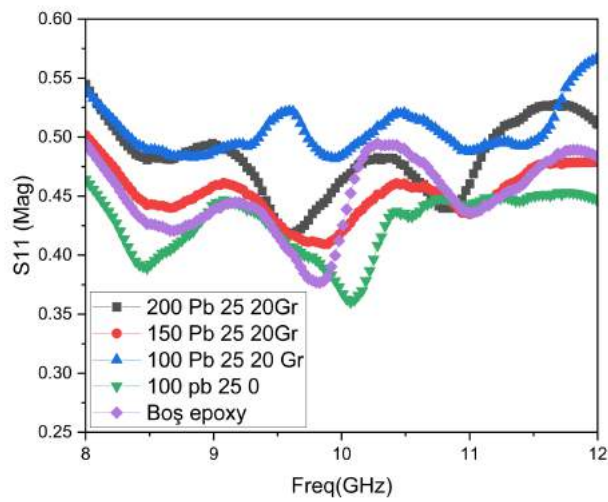


Figure 4.21: S_{11} and S_{21} for constant amounts of Graphite with changing amounts of PbO_2 with particle size below 25 microns inside the epoxy.

Constant Amount of Graphite with Changing Amount of PbO_2 (above 75 micron)

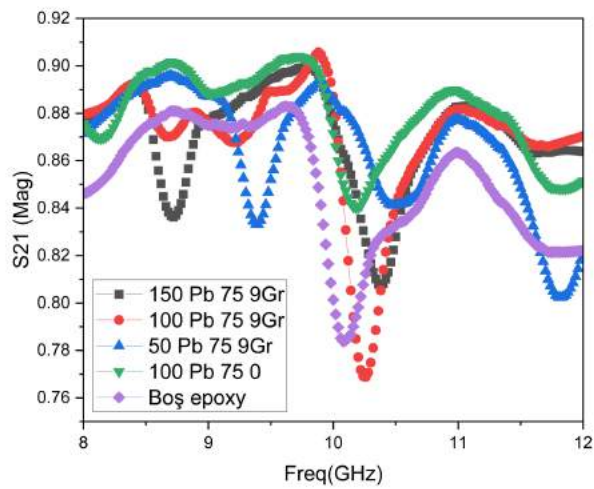
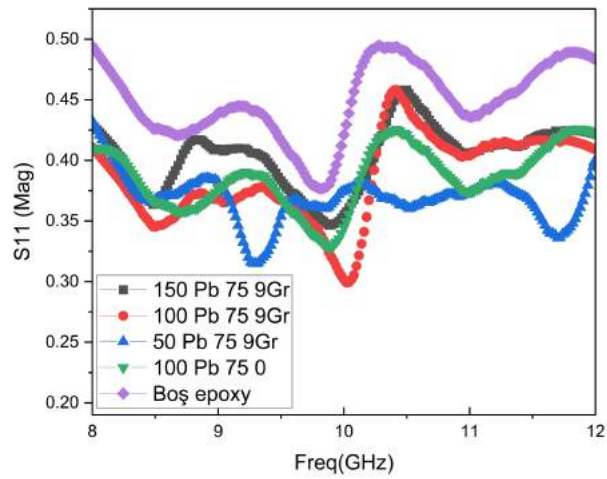


Figure 4.22: S_{11} and S_{21} for constant amounts of Graphite with changing amounts of PbO_2 with particle size above 75 micron inside the epoxy.

Constant Amount of Coal with Changing Amount of PbO_2 (below 25 micron)

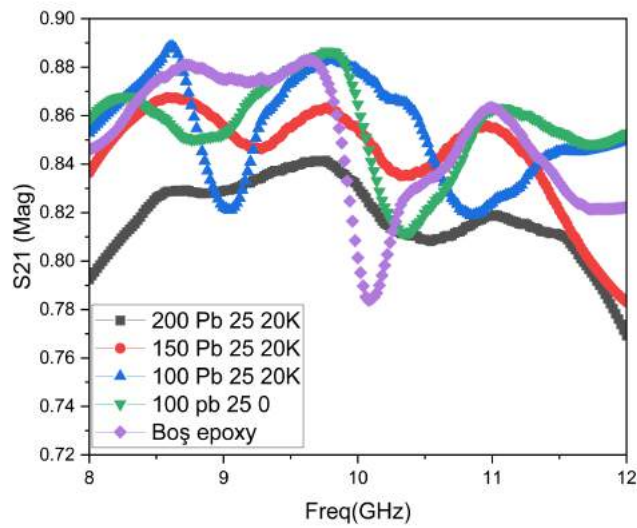
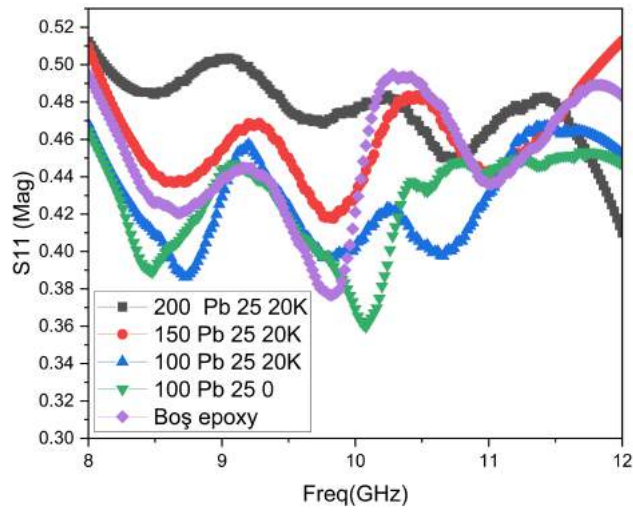


Figure 4.23: S_{11} and S_{21} for constant amounts of coal with changing amounts of PbO_2 with particle size below 25 microns inside the epoxy.

Constant Amount of Coal with Changing Amount of PbO_2 (above 75 micron)

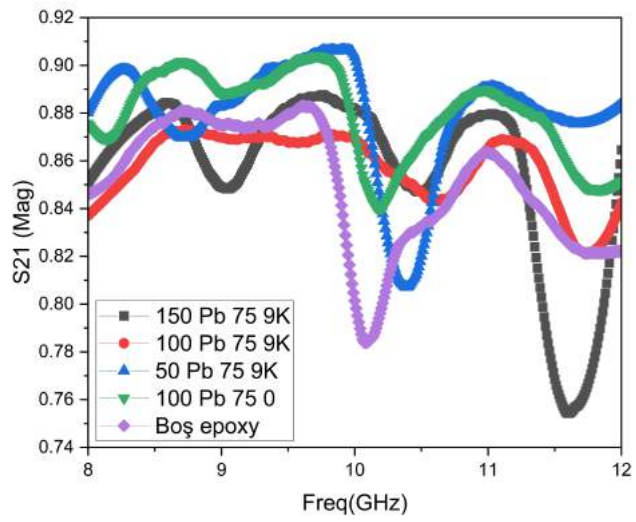
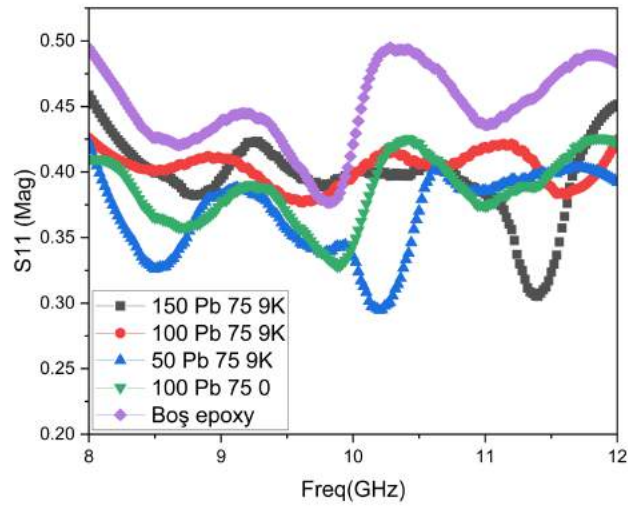


Figure 4.24: S_{11} and S_{21} for constant amounts of coal with changing amounts of PbO_2 with particle size above 75 microns inside the epoxy.

Constant Amount of PbO₂ (below 25 micron) with changing amount of Graphite

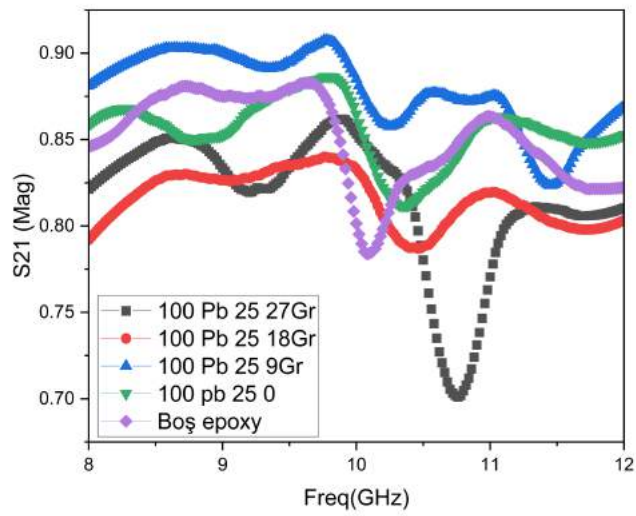
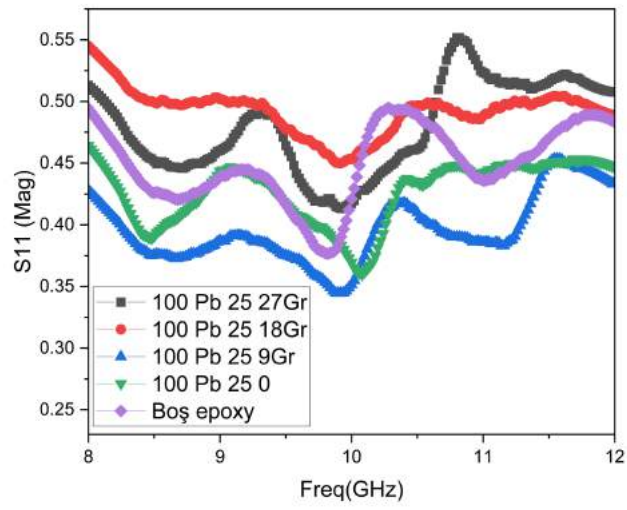


Figure 4.25: S₁₁ and S₂₁ for changing amounts of graphite with constant amounts of PbO₂ with particle size below 25 microns inside the epoxy.

Constant Amount of PbO₂ (below 25 micron) vs. changing amount of Coal

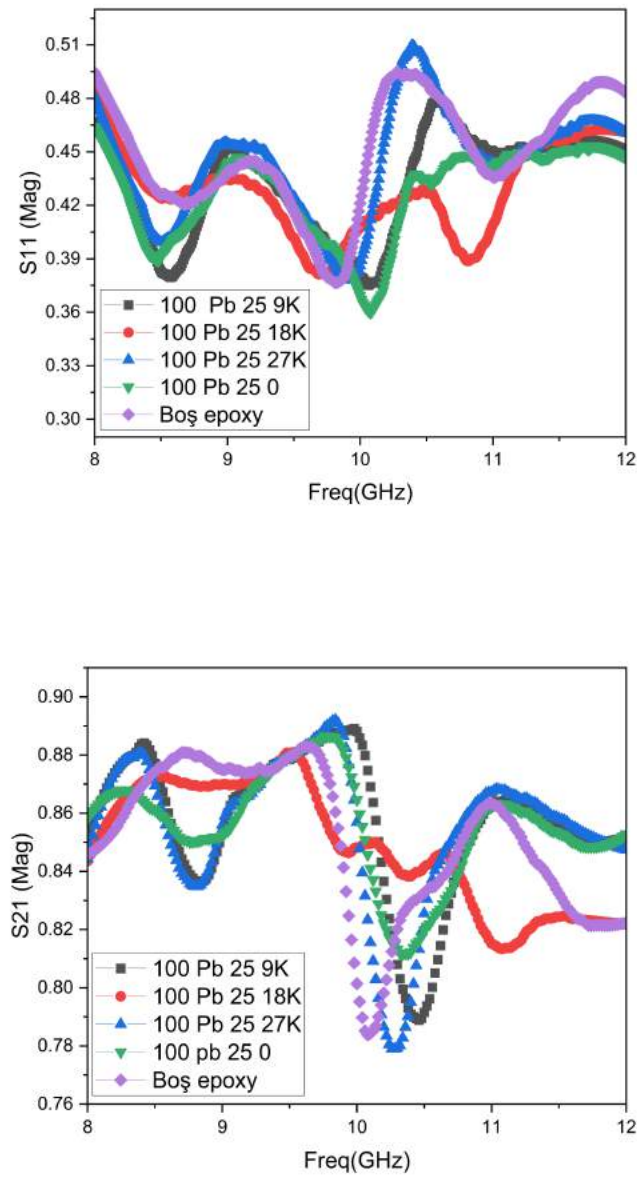


Figure 4.26: S₁₁ and S₂₁ for changing amounts of coal with constant amounts of PbO₂ with particle size below 25 microns inside the epoxy.

Constant Amount of PbO₂ (above 75 micron) vs. Changing Amount of Graphite

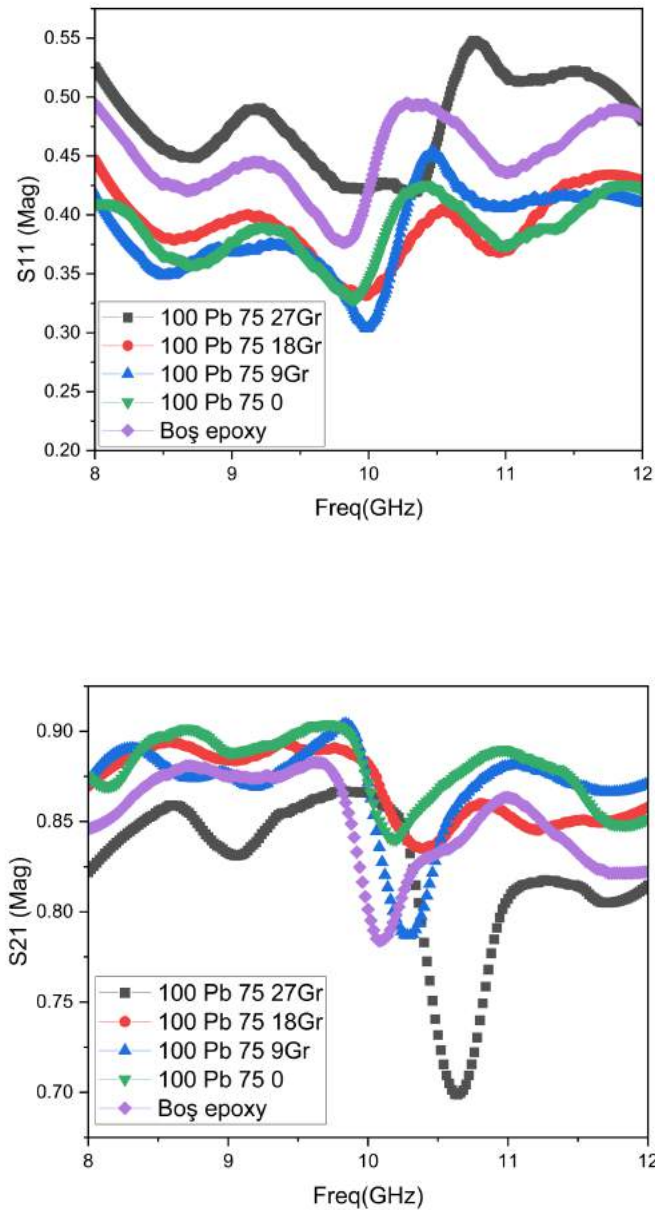


Figure 4.27: S₁₁ and S₂₁ for changing amounts of graphite with constant amounts of PbO₂ with particle size above 75 microns inside the epoxy.

The absorption was improved between 20 % and 25 %. The reflection loss decreased at the same rate. The graphite was better absorber than coal. Dielectric index of epoxy affects reflectivity in an adverse way.

Chapter 5

Conclusion

This thesis focused on the utilization of lead oxide as a radar absorbing material (RAM) and investigated its performance in terms of reflection loss (S_{11}) and transmission rate (S_{21}) within the X band frequency range of 8-12 GHz. The findings revealed that lead oxide exhibited an excellent reflection loss, indicating its potential for effective radar absorption. However, it was also observed that lead oxide transmission rate, which posed a challenge in achieving optimal absorption. To address this limitation, the study explored the incorporation of carbon-based materials such as coal and graphite into the RAM samples.

The addition of carbon-based materials aimed to enhance absorption capabilities by reducing the transmission of radar waves through the material. The results showed that the inclusion of coal and graphite indeed led to an increased absorption of the RAM samples. This improvement was achieved by decreasing the transmission of radar waves, thus increasing the energy dissipation within the material.

However, an unintended consequence of this enhanced absorption was the simultaneous increase in reflection of the RAM samples. This means that while the samples absorbed more radar energy, they also reflected a greater portion of the incident waves back towards the source. This phenomenon can be attributed to the different electromagnetic properties of the carbon-based materials compared to lead oxide.

The increased reflection could potentially have implications for the overall stealth performance of the RAM. The ability to absorb radar waves while minimizing reflection is crucial for reducing the detectability of an object or surface. Therefore, further

research and optimization are necessary to find a balance between absorption and reflection characteristics.

In conclusion, this study demonstrated that lead oxide possesses favorable reflection loss within the X band frequency range. However, its high transmission rate poses a challenge for effective radar absorption. The incorporation of carbon-based materials, such as coal and graphite, proved to enhance absorption but resulted in increased reflection. Future research should focus on finding ways to mitigate the unintended increase in reflection while maintaining or improving absorption capabilities. These findings contribute to the ongoing efforts to develop advanced radar absorbing materials with improved performance and reduced detectability.

References

- [1] Skolnik, M. I. (2008). Introduction to radar systems. McGraw-Hill.

- [2] Richards, M. A., & Scheer, J. A. (2018). Principles of modern radar: basic principles. SciTech Publishing.

- [3] Brown, R. G. (1956). The principles of FMCW radar. IRE Transactions on Aerospace and Electronic Systems, 2(3), 121-128.

- [4] Hofmann-Wellenhof, B., Lichtenegger, H., & Wasle, E. (2008). GNSS—Global Navigation Satellite Systems: GPS, GLONASS, Galileo, and more. Springer Science & Business Media.

- [5] Doviak, R. J., & Zrnić, D. S. (2006). Doppler radar and weather observations. Academic Press.

- [6] Ruffa, J. A., & Bott, M. H. (1984). Marine navigation and safety of sea transportation. Springer Science & Business Media.

- [7] Wang, X., & Ma, L. (2018). Dielectric materials for radar absorption. Progress in Electromagnetics Research, 161, 1-18.

- [8] Kundu, A., & Banerjee, D. (2017). A review on electromagnetic interference shielding properties of metal and carbon-based materials. Journal of Materials Science, 52(22), 12945-12978.

- [9] Skolnik, M. I. (2008). Radar handbook (3rd ed.). McGraw-Hill.

- [10] Li, L., Li, Y., Chen, W., Li, X., & Zhang, Q. (2019). Electromagnetic properties and applications of radar absorbing materials: A review. Journal of Materials Science & Technology, 35(1), 1-14.

- [11] Ropp, R.C. (2013). Encyclopedia of the Alkaline Earth Compounds. Elsevier.
- [12] Allen, G.C. (1999). Chemical Additives for Plastics. Springer.
- [13] Linden, D. and Reddy, T.B. (eds.) (2002). Handbook of Batteries. McGraw-Hill.
- [14] Agency for Toxic Substances and Disease Registry. (2007). Toxicological Profile for Lead. U.S. Department of Health and Human Services.
- [15] Geller, S. (1954). "The crystal structures of alpha and beta lead oxide". Acta Crystallographica 7 (8): 566–571.
- [16] “Qualitative lead extraction from recycled lead–acid batteries slag.” Alessandra Smaniotto^a, Angela Antunesa^a, Irajá do Nascimento Filho^c, Luciana Dornelles Venquiarutoa^a, Débora de Oliveirab¹, Altemir Mossib¹, Marco Di Lucciob¹, Helen Treichelb^{*}, Rogerio Dallago (Journal of Hazardous Materials 172 (2009) 1677–1680)
- [17] 2018 Wiley Periodicals, Inc. J. Appl. Polym. Sci. 2019, 136, 47241.
- [18] “Polymer matrix composites as broadband radar absorbing structures for stealth aircrafts” C. G. Jayalakshmi^{1,2}, A. Inamdar², A. Anand¹, B. Kandasubramanian (J. APPL. POLYM. SCI. 2019, DOI: 10.1002/APP.47241)
- [19] Trujillo A.P. & Thurman, H.V. The Black Arts: Materials and Process Selection and Stealth Technology. Essentials of Oceanography. (2004).
- [20] Tzu-Hao Ting, Kuo-Hui Wu, Jen-Sung Hsu, Ming-Ho Chuang, Cheng-Chien Yang. Microwave Absorption and Infrared Stealth Characteristics of Bamboo Charcoal/Silver Composites Prepared by Chemical Reduction Method. Journal of the Chinese Chemical Society. 55, 724-731(2008).

- [21] "A comparison on radar absorbing properties of nano and micro-scale barium hexaferrite powders reinforced polymeric composites", Hüsüngül Yılmaz ATAY (Mugla Journal of Science and Technology, Vol 2, No 1, 2016, Pages 88-92)
- [22] M. Golio and C. Golio, "Scattering Parameters and Network Analyzer Measurements," in RF and Microwave Passive and Active Technologies, 2nd ed. Boca Raton, FL: CRC Press, 2018, pp. 51-74.
- [23] D. Pozar, Microwave Engineering, 4th ed. Hoboken, NJ: Wiley, 2012.
- [24] K. Chang, RF and Microwave Circuit Design for Wireless Communications, 2nd ed. Hoboken, NJ: Wiley, 2011.
- [25] G. Gonzalez, Microwave Transistor Amplifiers: Analysis and Design, 2nd ed. Upper Saddle River, NJ: Prentice Hall, 1997.
- [26] "Electrochemically modified carbon fibers as an active mass additive in enhanced flooded lead acid battery" PhD Thesis, Alper Turhan. (Tez no: 641331)
- [27] V. M. Donnelly, M. J. Kennedy, and C. M. O'Mahony, "A review of particle size analysis techniques for the characterization of radar absorbing materials," Measurement Science and Technology, vol. 25, no. 9, pp. 1-18, 2014.
- [28] J. H. Qu, W. Z. Yan, X. Y. Zhang, and X. H. Lu, "Influence of Particle Size on the Microwave Absorbing Properties of Fe- Based Powders," Materials Science Forum, vol. 610-613, pp. 1005-1010, 2009.
- [29] S. A. Ganiev, B. A. Abdullaev, and T. D. Salakhov, "Effect of particle size and concentration on the electromagnetic absorption of composite materials containing iron powder," Journal of Magnetism and Magnetic Materials, vol. 322, no. 13, pp. 1901-1906, 2010.

- [30] J. L. Huang, J. H. Xu, L. Y. Meng, J. L. Gong, and Y. H. Zhao, "The effect of particle size on the microwave absorption properties of carbon black/silicone rubber composites," *Journal of Applied Polymer Science*, vol. 119, no. 2, pp. 758-764, 2011.
- [31] M. Wu, C. M. Liu, L. P. Qian, and X. Y. Li, "Effect of particle size and content on the electromagnetic properties of carbonyl iron/epoxy resin composite materials," *Journal of Magnetism and Magnetic Materials*, vol. 324, no. 1, pp. 41-47, 2012.
- [32] J. P. Singh and M. Kumar, "X-ray diffraction studies of radar absorbing materials: A review," *Journal of Materials Science: Materials in Electronics*, vol. 28, pp. 5361-5371, 2017.
- [33] Y. L. Tian, Y. B. Fan, and W. Liu, "Synthesis and characterization of core-shell structured carbonyl iron/expanded graphite composites for microwave absorption," *Journal of Alloys and Compounds*, vol. 797, pp. 1-8, 2019.
- [34] H. Lu, J. Yu, and C. Lai, "Influence of structural defects on microwave absorption of CoNi nanocrystalline alloys," *Materials Characterization*, vol. 161, pp. 110161, 2020.
- [35] S. Saravanan, S. Sankar, and K. Balasubramanian, "Investigation of structural and magnetic properties of ball milled cobalt ferrite nanoparticles for microwave absorbing applications," *Journal of Magnetism and Magnetic Materials*, vol. 496, pp. 165930, 2020.
- [36] "Preparation of high-purity lead oxide from spent lead paste by low temperature burning and hydrometallurgical processing with ammonium acetate solution" Cheng Ma, Yuehong Shu, Hongyu Chen. *RSC Advances*. 2016.
- [37] Elsherbeni, A. Z., & Al-Rizzo, H. M. (2012). *Electromagnetic scattering and radiation: numerical simulations*. Morgan & Claypool Publishers.

- [38] Ulaby, F. T., Moore, R. K., & Fung, A. K. (2014). *Microwave remote sensing: active and passive*. CRC Press.
- [39] Kanda, M. (1992). Electromagnetic wave absorption properties of carbonyl iron-silicone resin composites. *Journal of Applied Physics*, 71(1), 500-502.
- [40] Choudhury, P., & Jadavpur University. (2008). *Microwave absorber using nanocomposites: design, fabrication, and characterization*. Jadavpur University.
- [41] Cao, M. S., & Xie, X. M. (2011). Advanced composite materials for broadband electromagnetic absorption shielding. *Materials Science and Engineering: R: Reports*, 72(3), 51-72.
- [42] Wu, D., Chen, W., Chen, Y., & Wu, S. (2016). Bandwidth controllable electromagnetic wave absorption by graphene/iron hybrid structure. *Scientific Reports*, 6, 36960.
- [43] Wu, J., & Zhang, Q. (2011). Influence of Particle Size on the Color of Pigments. *Journal of the American Ceramic Society*, 94(11), 3789-3795.
- [44] Xia, Y., & Xia, X. (2011). Color Control of Colloidal Metal Nanocrystals. *ACS Nano*, 5(5), 3725-3734.
- [45] Pathak, N. N. (2017). *Radar absorbing materials: Design, simulation, and characterization (Vol. 45)*. Cambridge, MA: Academic Press.
- [46] Novoselov, K. S., Jiang, D., Schedin, F., Booth, T. J., Khotkevich, V. V., Morozov, S. V., & Geim, A. K. (2005). Two-dimensional atomic crystals. *Proceedings of the National Academy of Sciences*, 102(30), 10451-10453.
- [47] Aksamija, Z., Zhang, X., & Ruan, X. (2019). Graphene as a 2D material for defense applications. In *Handbook of Graphene* (pp. 1-22). CRC Press.

- [48] Ansoft. (n.d.). Radar Cross Section (RCS) Analysis and Simulation. Retrieved from://www.ansys.com//media/ansys/corporate/resourcelibrary/brochure/analytics-emea/ansys-rcs-analysis-and-simulation-datasheet.pdf
- [49] P. Chen et al., "Graphene and graphene-based composites for electromagnetic interference shielding," *Adv. Mater.*, vol. 28, no. 29, pp. 6211-6231, 2016.
- [50] S. Thomas, "Recent advances in electrically conducting polymers and composites," *Prog. Polym. Sci.*, vol. 29, no. 3, pp. 183-215, 2004.
- [51] H. Zhang et al., "Electromagnetic wave absorption properties of carbon nanotubes/silicon carbide composites," *Carbon*, vol. 48, no. 13, pp. 3892-3898, 2010.
- [52] Mario Costa Sousa, John W. Buchanan, "Observational Models of Graphite Pencil Materials," *Computer Graphics*, vol. 19, 2001.

Curriculum Vitae

Name Surname : Gürkan Ergün

Education:

2001–2005 İzmir Institute of Technology, Physics.

2008–2011 Stuttgart University, International Physics Master Programme.

Work Experience:

2006 – 2007 Ulm University

2009 – 2010 Stuttgart University, 5th Institute of Physics

2010 – 2011 Max Planck Institute, Solid State Research

2013 – ... İzmir Katip Çelebi University, Engineering Sciences